Composites Part C: Open Access 8 (2022) 100271

Contents lists available at ScienceDirect

Composites Part C: Open Access

journal homepage: www.sciencedirect.com/journal/composites-part-c-open-access

# A Review of 3D/4D Printing of Poly-Lactic Acid Composites with Bio-Derived Reinforcements

Lakshmi Priya Muthe *, Kim Pickering, Christian Gauss

*School of Engineering, The University of Waikato, Hamilton, New Zealand*

ARTICLE INFO

*Keywords:*
Polylactic acid
Bio-derived composites
Natural fibres
Thermoplastics
Additive manufacturing

ABSTRACT

Poly-lactic acid (PLA) has become a commonly used polymer for additive manufacturing because of its bio-derived nature, useful mechanical properties, and excellent processability. Reinforcing PLA with bio-derived materials has been shown to improve the physical, mechanical, and thermal properties of 3D printed composites and, in some cases, to produce active materials for shape-changing hygromorphic structures. PLA also displays shape memory as a response to changes in temperature, making it a popular choice for 4D printing. This review aims to present an overview of the current state of 3D/4D printing PLA composites with bio-derived reinforcements and highlight the recent progress and future opportunities. This comprehensive overview summarises the different forms of bio-derived reinforcements for PLA used in fused deposition modelling (FDM), factors influencing the resulting printed composites' performance, and research gaps that need addressing. The current methods used before, during, and after printing to enhance the material properties and the impending need for innovative filament production and printing technologies have been brought to attention.

## 1. Introduction

### 1.1. 3D and 4D Printing

Additive manufacturing (AM), also known as 3D printing, enables the fabrication of complex geometries, consolidation of sophisticated assemblies, customisation of products, and reduction of material waste [1]. These advantages have supported massive growth in the 3D printing market in the past few years. There has also been a significant increase in the number of publications related to 3D printing in the last decade (Figure 1), primarily distributed in the areas of engineering, materials science, physics and astronomy, computer science, and chemistry, with a total of 78,624 documents between 2010 to 2021.

3D printing is an additive process in which a three-dimensional object is created from a digital model by adding material, typically in successive layers. 3D printing can be contrasted with traditional manufacturing processes that use subtractive approaches such as machining, grinding, and casting, where molten material is filled in a mould to create a product [2]. There are various types of 3D printing technologies, and all of them have their targeted applications. According to ASTM standard F2792, 3D Printing, or AM technologies, are grouped into seven categories: binder jetting, directed energy deposition, material extrusion, material jetting, powder bed fusion, sheet lamination and vat photopolymerisation, as shown in Figure 2 [3].

*Binder Jetting*

Binder jetting involves a technique like that of inkjet technology used in a typical desktop inkjet printer. An inkjet printer head selectively deposits the liquid binder on the powder spread in this process. It is an energy-efficient process as it does not use heat to bind the materials. Additionally, all the unused powder is fully recyclable as the powder is not heated. Metals, polymers, and ceramics are commonly used materials in this technique [3–5].

*Directed energy deposition*

DED is used to create objects using focussed heat input to fuse the material that is deposited in a layer by layer fashion with a multi-axis nozzle. Types of heat inputs used for DED include laser, electron beam, and arc [6]. The material feedstock is in the form of powder or a wire. DED is predominantly used for the repair of metal objects [7].

*Material Extrusion*

Fused deposition modelling (FDM) is an example of a material extrusion technique. In this method, thermoplastic filaments are first

* Corresponding author
*E-mail address:* lm242@students.waikato.ac.nz (L.P. Muthe).

https://doi.org/10.1016/j.jcomc.2022.100271

Available online 27 April 2022

heated and then extruded through a nozzle tip. The extruded molten material is then added layer after layer following the digital model of the part. FDM is mostly applied when creating concept models in the early stages of product development to reduce costs and shorten production time. The advantage of FDM is that the filament materials are readily available. In addition, a wide range of FDM filaments exists with different strengths and temperature properties [8].

*Material jetting*

Material jetting is similar to a traditional inkjet printer in its principle of operation. In this process, photopolymer droplets are deposited precisely on the build surface. The build platform height changes to repeat the deposition after the previously deposited material solidifies. A wide range of materials, including composites, polymers, and ceramics, are used in this process [3,5]

*Powder bed fusion*

PBF uses high power energy sources to melt or sinter deposited material layers to form a single object. Electron beam melting (EBM), selective laser melting (SLM), and selective laser sintering (SLS) are three different types of PBF methods based on the type of power source [6]. Various classes of materials, including metals, synthetic polymers, and ceramics, can be used for PBF [7].

*Sheet lamination*

Sheet lamination differs from other 3D printing processes in using sheets as material feedstock instead of powder or wire. In this method, precision-cut layers of metal or polymer are stacked layer by layer and are bonded by diffusion to obtain the final object [9].

*Vat photopolymerisation*

VP is a 3D printing method where photoreactive materials are cured using a light source or ultraviolet radiation in a controlled manner to form a 3D object. Stereolithography (SLA) and digital light processing (DLP) are examples of VP. DLP uses an arc lamp as a light source, whereas SLA uses ultraviolet light [3]. Stereolithography is the most precise AM technology, so it is used in creating high-quality prototypes with complex and intricate geometrical shapes. It also can produce objects with high dimensional tolerance and an excellent surface finish. However, the high amount of resins used increases the cost of stereolithography technology [8].

Although most 3D printing methods use a layer-by-layer manufacturing method, an innovative method named 3D freeform printing has been used to build complex geometries in open space with a robotic arm that houses an extrusion chamber. The robotic arm extrudes and places the material where required in a three-dimensional place to produce the final object [13,14]. A comparison of the number of publications between 2010 and 2021 for the most commonly used 3D printing methods is shown in Figure 3, where FDM, a material extrusion process, has the highest number of publications with a total of 3,102 documents between 2010 and 2021. A variety of materials, including metals, polymers, resins, and powders, are used for 3D printing [15]. Polymers are the most commonly used materials, including thermoplastics, thermosets, hydrogels, functional polymers, and polymer-based composites [16,17].

Four-dimensional (4D) printing, derived from 3D printing, involves manufacturing objects engineered to react to an external stimulus in a useful way [1]. 4D printing utilises smart materials programmed to exhibit changes in one or more properties in a controlled manner on the application of an external stimulus [18] such as heat, light, water, or UV light [19]. Examples of such smart behaviours are self-sensing, self-healing, self-actuating, self-diagnostic, and shape-changing effects (see Table 1) [20]. 4D printing enables actuation in a material without the need for electromechanical systems, which can be translated into reduced expenditure, reduced need for assembly, and avoids the possibility of failure of electronic components [21,22].

An illustration of the difference between 3D and 4D Printing is shown in Figure 4. There are two main differences between 3D and 4D Printing - smart materials and smart design. In 4D printing, smart materials are programmed for predefined changes that occur post-printing, unlike in 3D Printing, where there the product is not expected to undergo any shape related changes post-printing. Consider the case of printing flat cardboard, which is programmed to turn into folded cardboard. Without a programmed smart material, a folded cardboard would be printed directly via 3D printing. In 4D printing technology, the flat object is printed first with a programmed smart material that can later

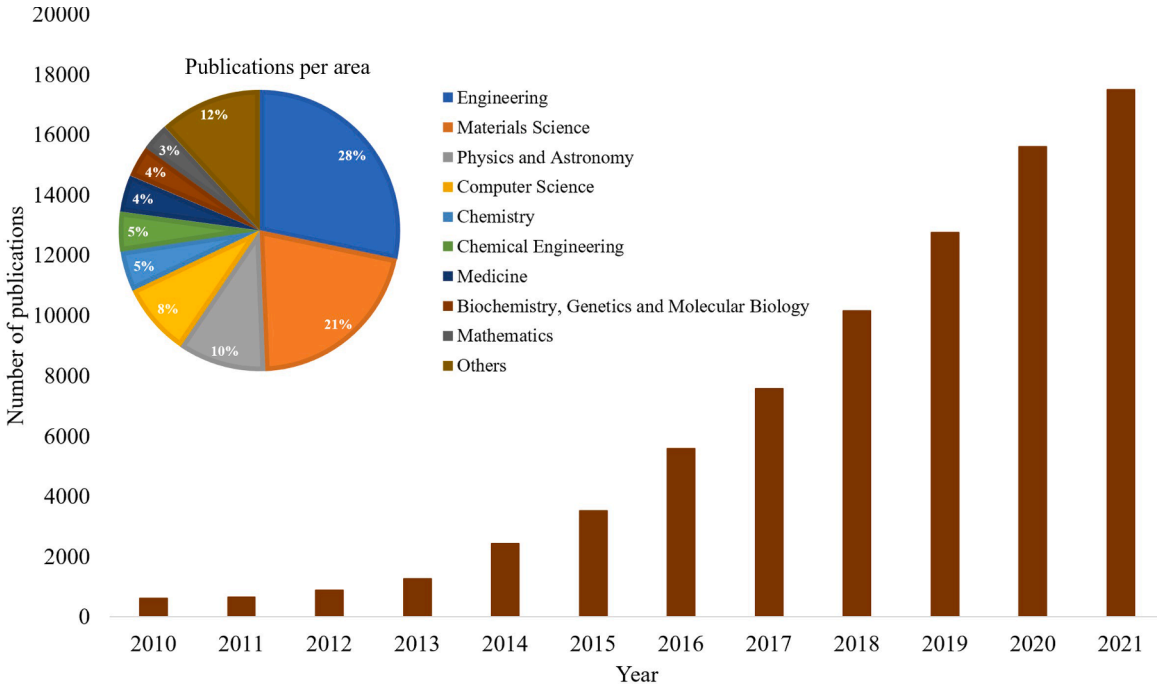


**Figure 1.** Number of publications in the Scopus database between 2010 and 2021 with the keywords: "3D printing" OR "additive manufacturing".

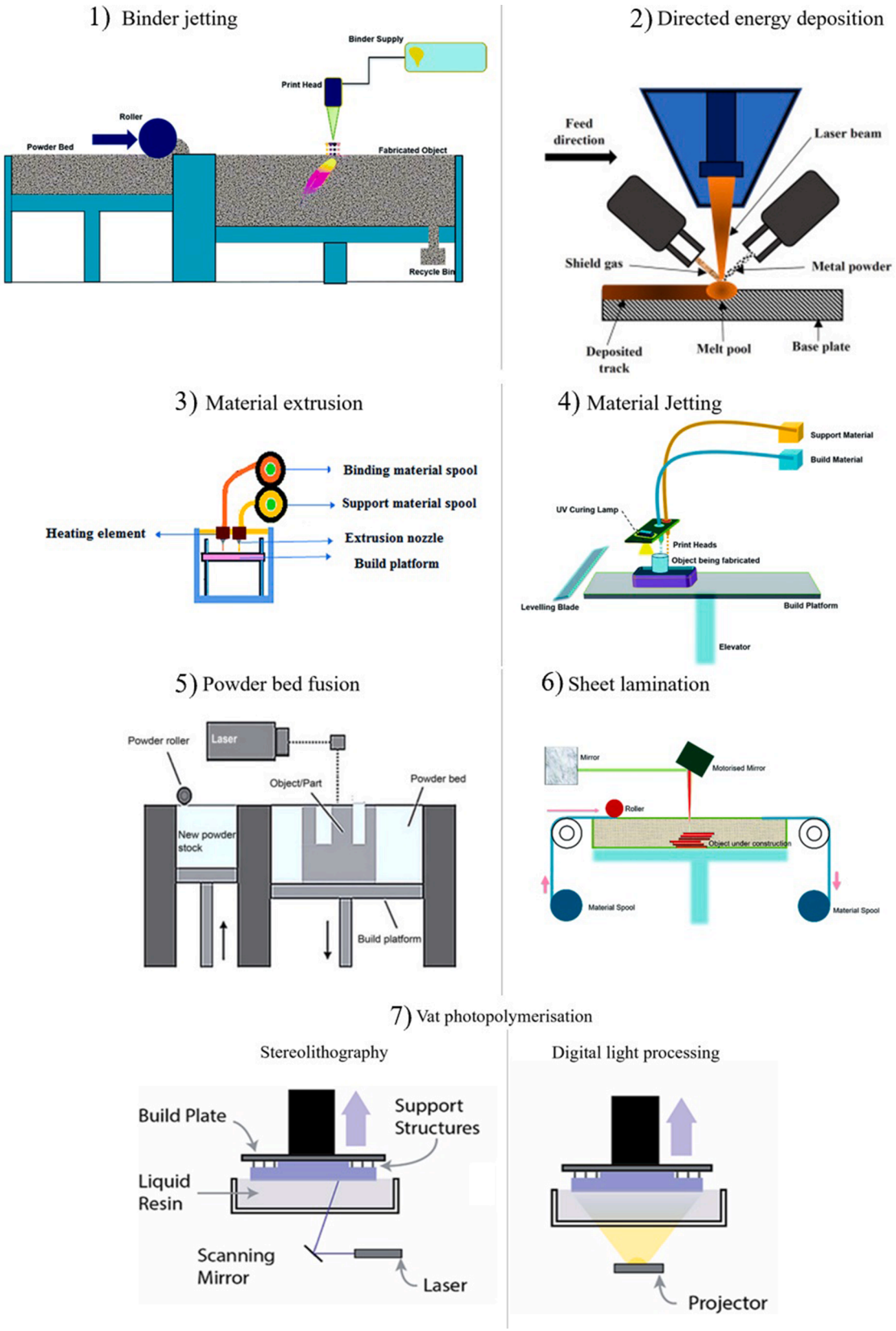


**Figure 2.** Types of 3D printing techniques as per ASTM standard F2792 1) Binder jetting: Reproduced from [10] with permission of Royal Society of Chemistry 2) Directed energy deposition: Reproduced with permission from Elsevier, license number 5279001041777 3) Material extrusion: Reproduced from [10] with permission of Royal Society of Chemistry 4) Material jetting: Reproduced from [10] with permission of Royal Society of Chemistry 5) Powder bed fusion: Reproduced with permission from Elsevier, license number 5279081324096 [11] 6) Sheet lamination: Reproduced from [10] with permission of Royal Society of Chemistry 7) Vat photopolymerisation [12].

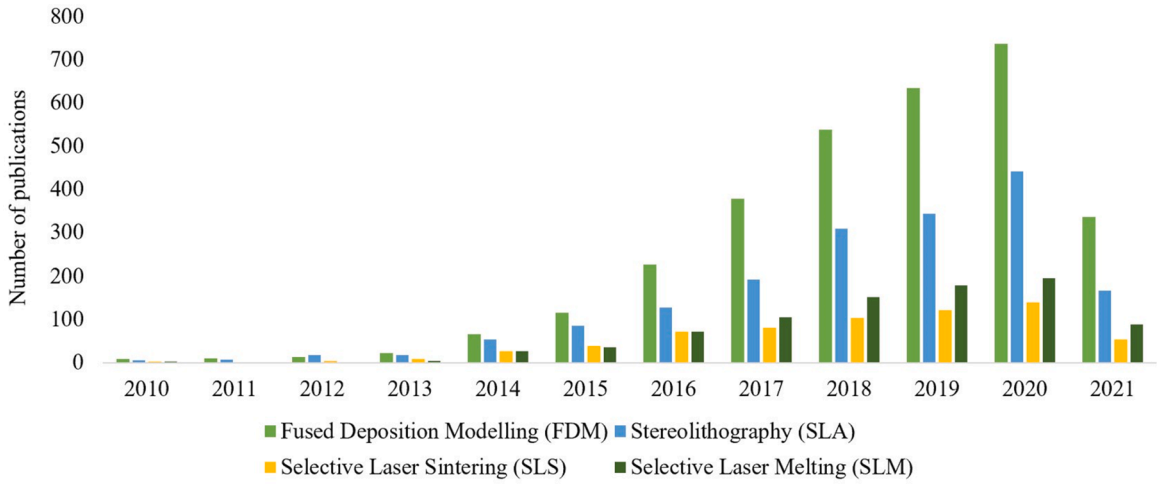


**Figure 3.** Number of publications in the Scopus database between 2010 and 2021 with the keywords: "3D printing" AND "fused deposition modelling"; "3D printing" AND "stereolithography", "3D printing" AND "selective laser sintering", and "3D printing" AND "selecting laser melting".

**Table 1**
Capabilities of smart materials used in 4D printing [20].

| Function | Description |
|---|---|
| Shape changing /shape memory | Material changes shape in response to external stimulus. |
| Self-assembly | Allows automated folding for assembly. |
| Self-actuating | Allows actuation in response to stimulus |
| Self-sensing | Allows automatic detection and sometimes quantification of external stimulus. |

perform self-transformation into a folded cardboard structure [23]. 4D printing technology can give more value to particular applications, while in 3D printing technology, there is scope for high quality and versatility with regards to applications and fabrication [24]. The potential uses of 4D printing technologies include applications in architecture, medicine, food, automotive, and other industries [25].

### 1.2. Bio-derived materials in 3D/4D Printing

There is increasing awareness in the 3D printing industry regarding sustainable alternatives to current materials [26]. According to statistics [27], thermoplastics (see Figure 5, where plastics refer to thermoplastics) are the most commonly used materials for 3D printing, and FDM is the most used technology [28]. However, extensive use of petrochemical-based thermoplastics does not align well with achieving a circular economy. Consequently, there has been a significant interest in incorporating bio-derived polymers and their composites as alternatives for conventional oil-based polymers to make the additive manufacturing industry more sustainable [29].

Poly (lactic acid) (PLA) is a bio-derived and biodegradable polymer that is the most used material worldwide for 3D printing, as shown in Figure 6 [26,30]. Other bio-derived polymers used for 3D printing include PHA (polyhydroxyalkanoates) [31,32], Bio PE (bio-derived polyethylene) [33], PEF (poly(ethylene-2,5-furandicarboxylate)) [34], Bio PC (bio-derived polycarbonate) [35], and Bio PA 11 (Polyamide 11)

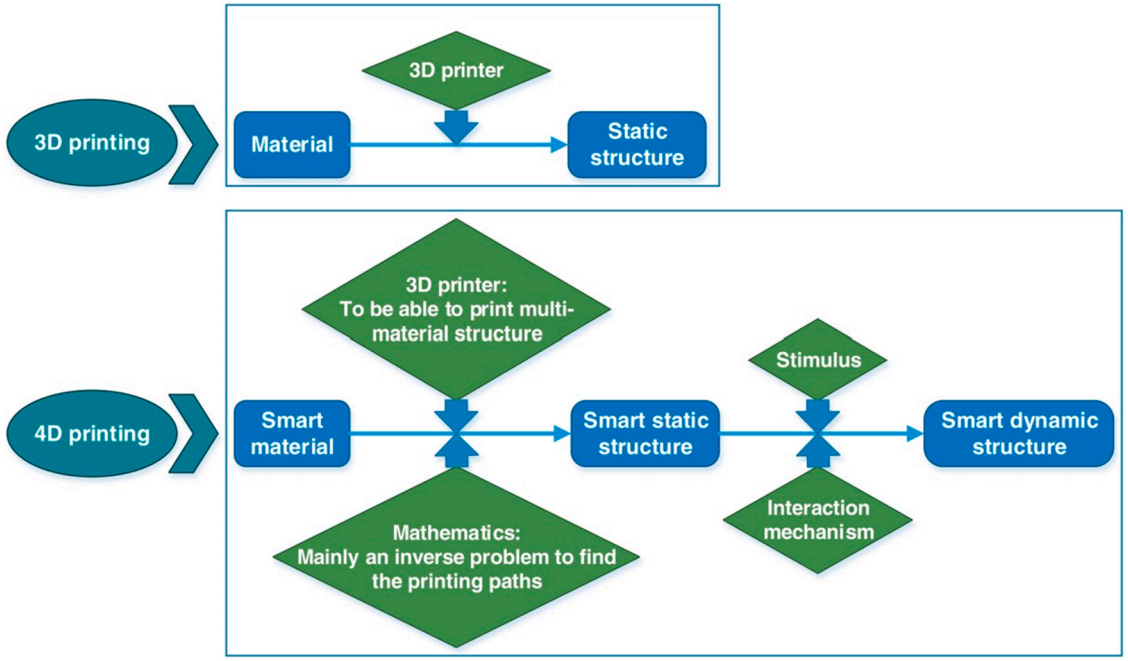


**Figure 4.** Difference between 3D and 4D printing [22]. Reproduced with permission from Elsevier, license number 5279100212677.

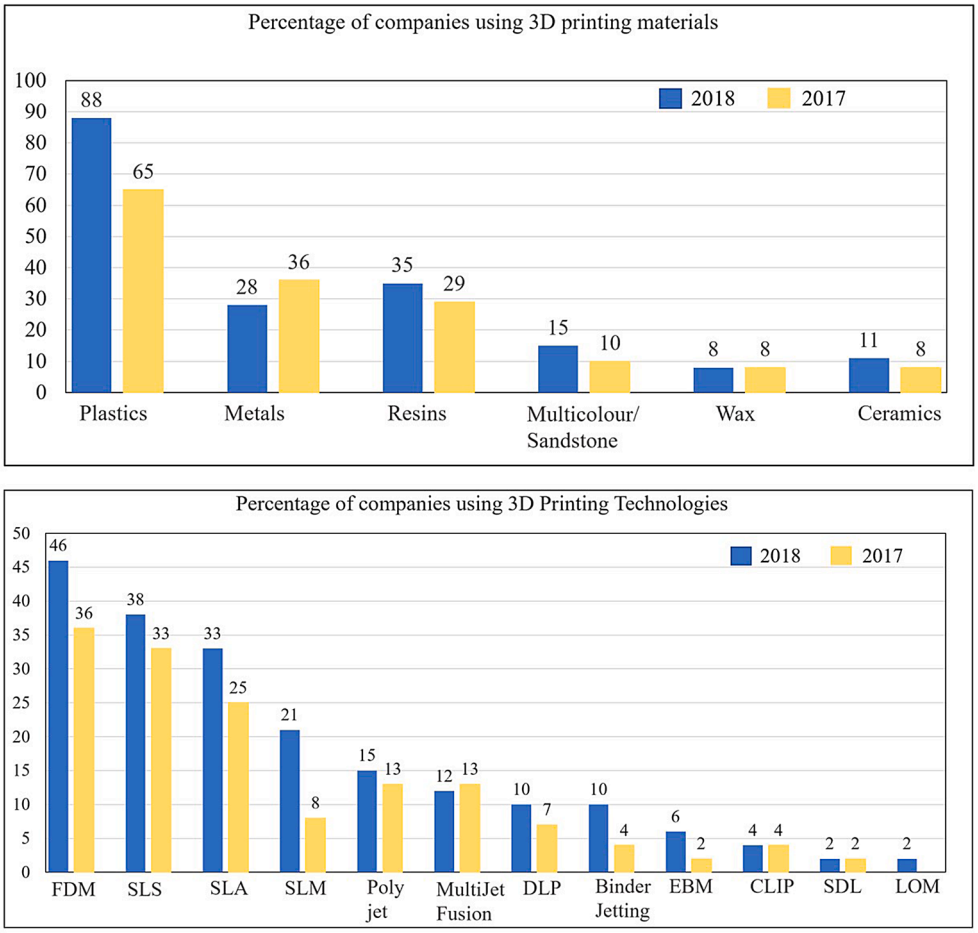


**Figure 5.** Percentage of companies using different 3D printing materials and technologies in 2017 and 2018 [27]. Where: FDM – Fused deposition modelling; SLS – Selective laser sintering; SLA – Stereolithography; SLM – Selective laser melting; DLP - Digital light processing; EBM – Electron beam melting; CLIP/CDLP – Continuous liquid interface production; SDL – Selective deposition lamination; LOM – Laminated object manufacturing.

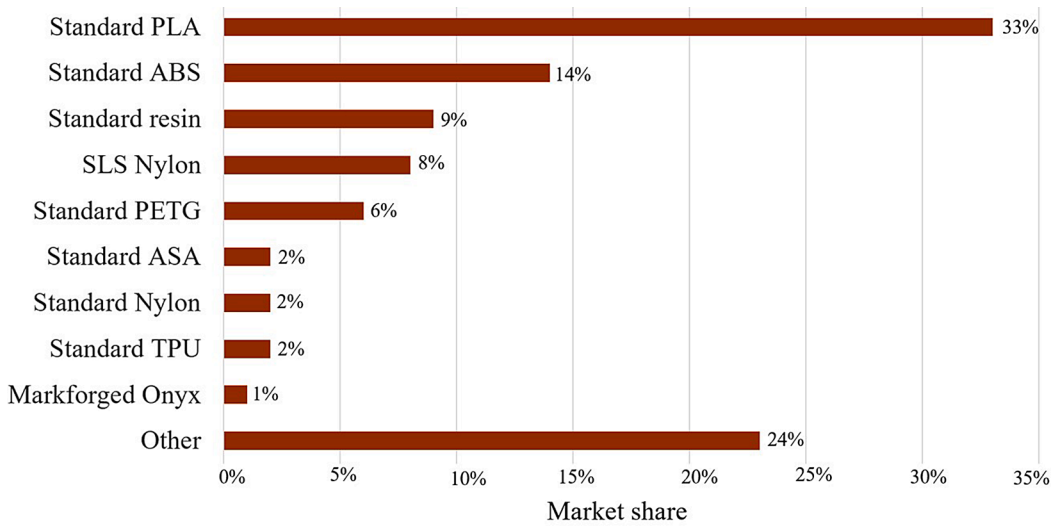


**Figure 6.** Worldwide most used polymers for 3D printing as of July 2018 [30].

[36] as shown in Table 2. PLA has the highest tensile and flexural strengths compared to other bio-derived thermoplastics used for 3D printing and is also preferred as it is more readily available [37].

PLA composites have been used for FDM 3D printing to achieve better mechanical properties and improved functionalities that are not obtained using PLA directly [44]. PLA composites with bio-derived reinforcements such as flax, hemp, jute, bamboo, and other natural fibres have been widely researched for 3D printing to enhance mechanical properties, reduce material and production cost, and improve the sustainability of manufactured products [45,46].

**Table 2**
Mechanical properties of bio-derived thermoplastics used in 3D printing.

| Biopolymer | Tensile strength (MPa) | Young's modulus (GPa) | Elongation at break (%) | Flexural strength (MPa) | Flexural modulus (GPa) | Biodegradability | Ref. |
|---|---|---|---|---|---|---|---|
| PLA | 50 - 89.1 | 3 - 4 | 2 - 9 | 120-150 | 3.5 - 5 | Biodegradable | [38] |
| PHA | 15 - 40 | 1 - 2 | 1-15 | 17 - 61 | 1.4 - 3.2 | Biodegradable | [31, 32] |
| Bio PE | 18.4 – 17.9 | 1.4 – 1.9 | 5 - 7 | 18.7 - 19.8 | 0.8 - 1.01 | Non-biodegradable | [39, 40] |
| PEF | 67 - 77 | 2.7 - 2.9 | 2 - 4 | - | - | Non-biodegradable | [41] |
| Bio PC | 70.23 – 75.13 | 2.3 – 2.5 | 16.48 – 93.84 | - | - | Non-biodegradable | [42, 43] |
| Bio PA 11 | 52 – 54 | 1.7 – 1.8 | 28 | - | - | Non-biodegradable | [36] |

4D printing of bio-derived polymers and their composites can be achieved using a bio-derived shape memory polymer (SMP) or by combining a bio-derived polymer with moisture sensitive natural fibre reinforcement. SMPs undergo a cycle involving two steps during their transformation. In the first step, the material is programmed to deform its shape from the original shape to a temporary shape. In the second step, an external stimulus is applied upon which the material recovers its original shape. The material's ability to recover its original shape is called the shape-memory effect [47,48]. PLA is an example of a bio-derived polymer used as a shape-memory polymer in 4D printing applications [49–52].

Another way for 4D printing bio-derived polymer composites is by exploiting the moisture responsive behaviour of natural fibres. Natural fibres are sensitive to moisture, and this property can be used to develop materials that actuate when exposed to moisture. Such motion is naturally observed in pine cones and wheat awns [53]. The principle of actuation in pinecones is based on differential swelling between two layers in the bilayer assembly of the plant cell wall. The plant's secondary cell wall consists of stiff cellulose fibrils in the hygroscopic hemicellulose and pectin matrix. Upon wetting, the hygroscopic matrix swells, and the presence of stiff cellulose fibrils constrains the swelling. Hence, differential swelling causes the pine cone to open [54].

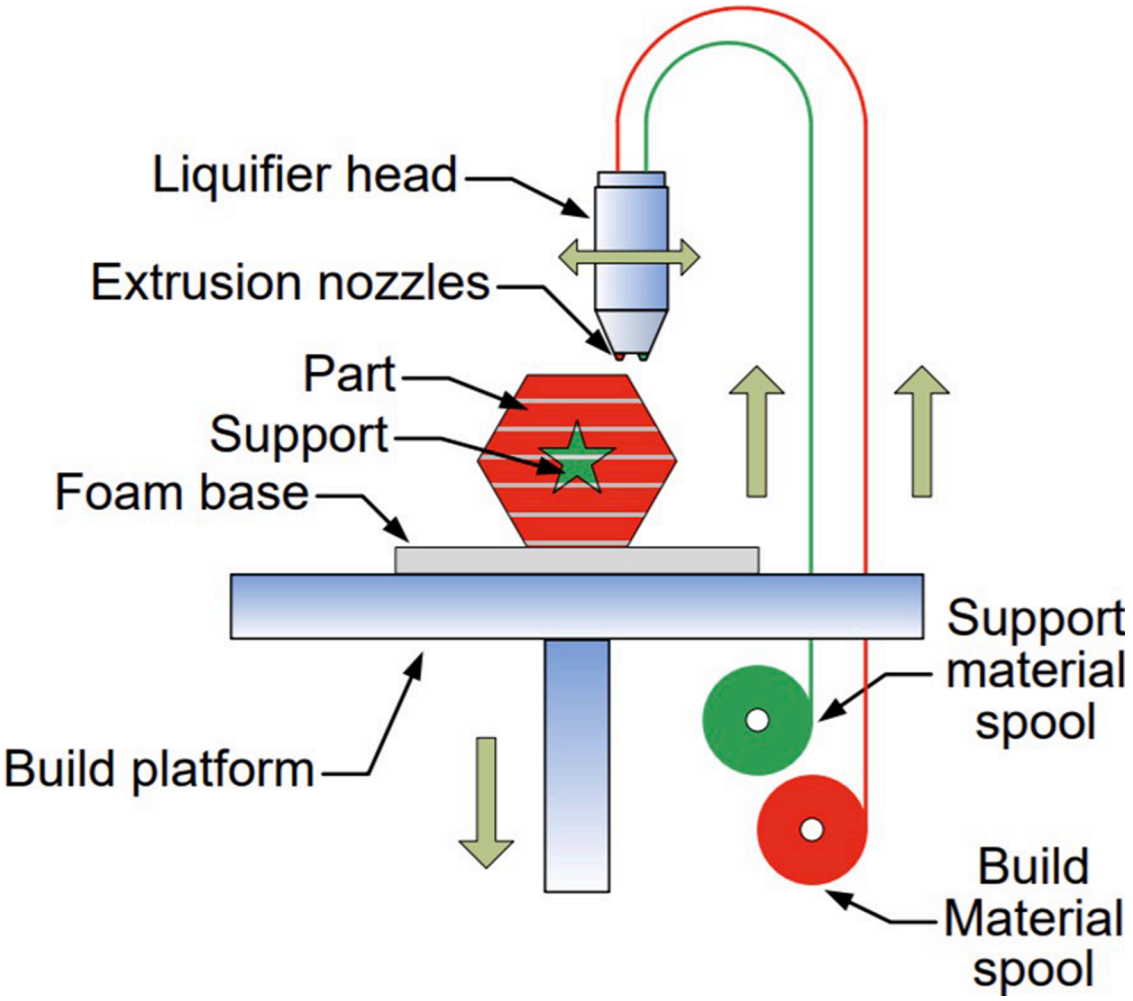


**Figure 7.** Schematic representation of fused deposition modelling method. Reproduced with permission from Elsevier, license number 5170280890406 [59].

## 2. Fused Deposition Modelling (FDM)

FDM, also referred to as fused filament fabrication (FFF) or material extrusion, is a 3D printing technique with various advantages, including low cost, moderate operating conditions, and large build volumes capacity [55–57]. On the other hand, it has disadvantages such as limited accuracy, slow printing speeds, and shrinkage due to temperature changes [56].

The FDM process (Figure 7) begins by digitally slicing the 3D CAD model into layers, and the data, converted to a G-code (Geometric code for computer numerical control), is transferred to the 3D printing machine, which constructs the part layer by layer. Next, both the support material and the thermoplastic filaments, generally with diameters of 1.75 or 3 mm, are fed into the heated chamber and melted. The molten material is then extruded through nozzles in a layer-by-layer structure. Finally, the finished part is removed from the build platform, and if necessary, the support material is removed [58].

Many studies have focused on the effects of FDM printing parameters on the performance of the 3D printed parts [55,60–63]. The parameters that affect an FDM printed part's quality include build orientation, raster angle, layer thickness, infill density, and extrusion temperature, as shown in Table 3 [64].

Build orientation is one of the most influential structural parameters in terms of the mechanical properties of FDM parts. Compared to parts printed in a perpendicular direction to the build platform, FDM parts printed in horizontal or vertical directions have a substantial decrease in mechanical properties [67–69]. Raster angle also influences the mechanical properties of FDM printed samples. Studies show that samples printed with a raster angle of 0° have the highest tensile properties, followed by 0°/90°, 45°/45°, and 90° [70–73]. Layer thickness and infill percentage are also important parameters that influence the quality and mechanical properties of FDM printed objects. Increasing layer thickness improves print time but reduces surface finishing. A layer thickness between 0.1 to 0.4 is considered optimum for most FDM applications [71,74,75]. An increase in infill percentage improves the tensile properties in FDM printed parts. Hence, most studies on improving the mechanical performance of FDM parts select an infill percentage of 100% [55,60,76]. However, low infill percentages are preferred for reducing time and cost.

Besides the effect of geometry-related parameters, extrusion temperature and printing speed also influence the properties of FDM printed parts. Higher temperatures have been shown to improve bonding between the layers; at high temperatures, the melt flow of the polymer is higher, which increases the interfacial area between the layers leading to a decrease in voids and an increase in mechanical performance. However, high temperatures also affect dimensional accuracy and cause shrinkage in some polymers [55]. Optimum printing speed in FDM is dependent on the material selected. In the studies related to the effects of printing speed on FDM parts, it has been observed that interlayer bonding between the filaments reduces with an increase in printing speed, which is attributed to the lack of time for polymer plasticisation [75,77–79].

## 3. Poly (lactic acid) (PLA) – Lifecycle, Synthesis, and Properties

PLA is a bio-derived thermoplastic polymer synthesised from lactic acid obtained from corn, sugarcane, and other biomass. It is also a 100% biodegradable polymer with high tensile strength and modulus. PLA can be recycled up to 8 times and is compostable at the end of life [80]. The life cycle of PLA is shown in Figure 8.

PLA is synthesised from lactic acid in three ways – direct polycondensation of lactic acid (LA), azeotropic dehydrative condensation, and ring-opening polymerisation (ROP) of lactide (Figure 9). ROP is the most commonly used method as it yields high molecular weight PLA and requires low temperatures and short reaction times [81,82]. First, low molecular weight oligomers are produced by the continuous condensation reaction of aqueous lactic acid. Followed by this, the oligomer or prepolymer is catalytically converted into cyclic lactide. This cyclic lactide production results in three forms: D,D-lactide (D-lactide), L,L-lactide (L-lactide) and L,D- or D,L-lactide (meso lactide) as shown in Figure 10 [83]. The next step is distillation, where impurities are removed, and meso lactide is separated. The final step involves the ROP of lactides to obtain different grades of PLA.

The stereochemical structure of PLA can be controlled by controlling the mixture of L- or D- isomers to obtain different proportions of crystalline and amorphous phases. The polymerisation of L-lactide produces poly (L-lactide) (PLLA), D-lactide produces poly (D-lactide) (PDLA), and racemic (50% L- and 50% D-) produces poly (DL-lactide) (PDLLA). PLLA and PDLA are optically pure polylactides and are crystalline, whereas PDLLA is amorphous. PLA can be degraded by simple hydrolysis without the use of enzymes to catalyse the hydrolysis [81].

The thermal, mechanical, and biodegradation properties of PLA depend on the distribution of the stereoisomers in the polymer chains. PLA with greater than 90% content of PLLA is highly crystalline, and a lower percentage of PLLA yields more amorphous PLA. Melting temperature ($T_m$) and glass transition temperature ($T_g$) of PLA increase with the increase of L-isomer content and decrease of D-isomer content [83].

## 4. FDM 3D Printing of PLA Composites with Bio-Derived Reinforcements

When particle, fibre, or flake reinforcements are embedded into a matrix material, the resultant material is defined as a composite. Most polymer-based composites have 60% to 70% polymers as their matrix, and the reinforcement material constitutes about 30% to 40% [86]. Reinforcement is considered the principal component in a composite system, with the primary function of improving the mechanical properties of the composite [87]. In this review, reinforcement is defined as the component that at least improves Young's modulus of the resulting composite when added to the polymer. Bio-derived reinforcements used in FDM 3D printing can be classified into micro (100 μm to 100 nm) and nano (100 nm to 1 nm) reinforcements which are further classified into fibre and particle reinforcements based on their shape and size, as shown in Figure 11. This classification is based on the forms of reinforcement used from a material processing perspective. Bio-derived micro fibre reinforcement forms are further classified into discontinuous and continuous, where single fibres and chopped fibre bundles are discontinuous reinforcement forms, and single fibres spun into yarns are continuous reinforcement forms [88]. Nano reinforcements are classified into nano fibre and nano particle reinforcements [89].

Bio-derived micro fibres are the most common type of reinforcements, and their sources can be both natural and man-made, as shown in Figure 12. While natural fibre reinforcements have been widely used for FDM 3D printing of PLA, man-made fibres have not been explored for FDM applications so far. Natural fibres include plant, animal, and mineral fibres [90]. Plant fibres are composed of cellulose, hemicellulose, and lignin and are categorised as wood, bast, leaf, straw, grass, and seed fibres. Animal fibres are constituted of protein and are classified into hair and silk. Mineral fibres are in the asbestos group of minerals and are not preferred due to their carcinogenic nature [91]. Man-made or regenerated cellulose fibres are classified into lyocell, viscose, and modal [92]. Production of regenerated cellulose fibres typically involves pre-treatment of cellulose with a solvent to swell the cellulose molecules and induce chain relaxation, followed by a spinning process. The viscose process is the oldest method to produce regenerated cellulose fibres, where derivatizing is used to modify cellulose, followed by dissolution and spinning. The process for obtaining modal fibres is similar to viscose, except the fibres undergo treatment after the spinning process to improve the molecular alignment thereby increasing the strength of the fibres. Lyocell fibres on the ither hand, are produced by a direct dissolution of cellulose using ionic liquids or N-methylmorpholine-oxide (NMMO). Lyocell process is relatively new and is

**Table 3**
Important printing parameters in FDM (adapted from [64–66]). Extrusion temperature: Reproduced with permission from Elsevier, license number 5166990649229; Infill density: Reproduced with permission from Elsevier, 5166991182219.

| Parameters | Description | Graphical representation |
|---|---|---|
| Build orientation | Orientation of the component with respect to the build platform. | 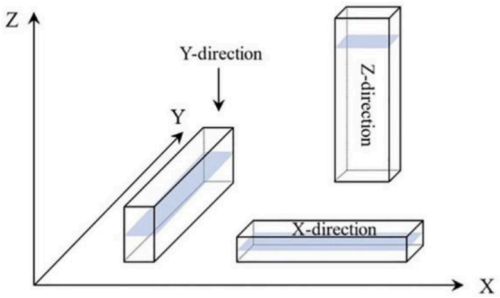  |
| Raster angle | The angle between the path of material deposition and the x-axis of the build platform. | 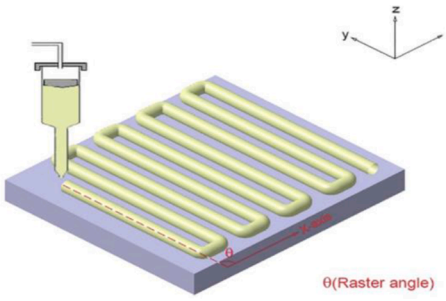  |
| Layer thickness | A measure of the layer height deposited by the nozzle. | 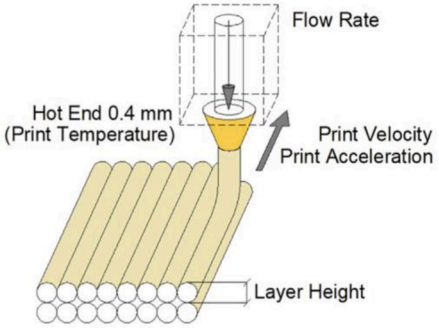  |
| Infill density | Material percentage filling the internal structure of the printed component. |   |
| Extrusion temperature | The temperature inside the nozzle before the material is extruded. | 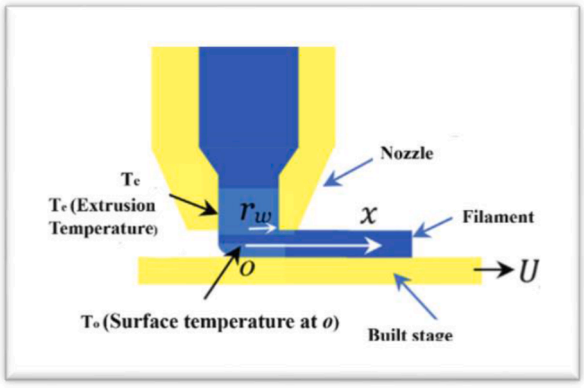  |

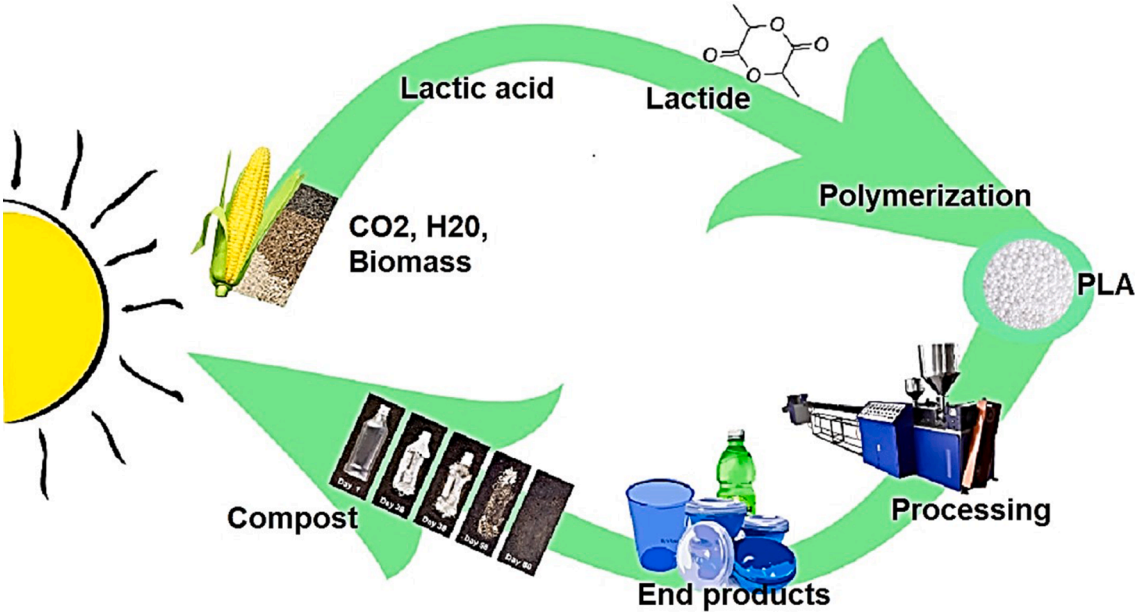


**Figure 8.** Life cycle of PLA.

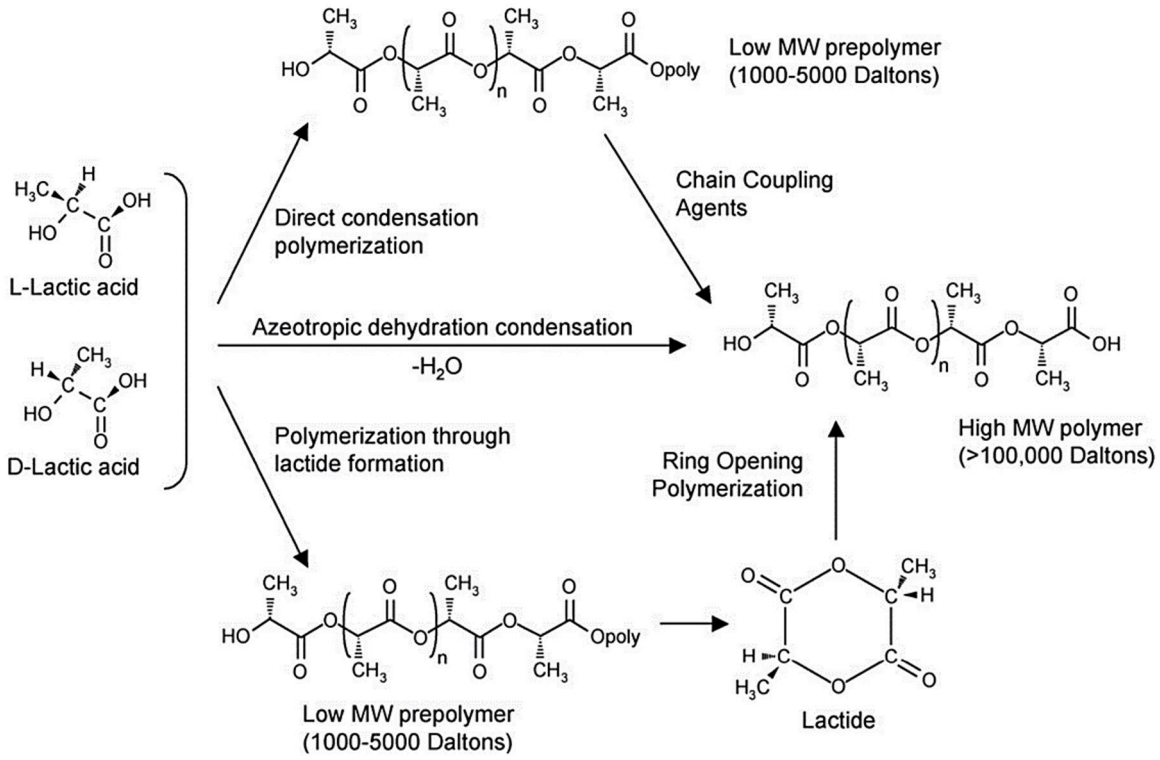


**Figure 9.** Methods of synthesising PLA from lactic acid [84] Reproduced with permission from Elsevier, license number 5124211449068.

considered environmentally friendly compared to viscose and modal processes due to the ability to recover more than 90% of the solvents used [93].

A list of properties of bio-derived fibres is given in Table 4. Flax, hemp, and ramie have the highest tensile strength and Young's modulus amongst the natural fibres. Animal fibres have low mechanical properties compared to other bio-derived fibres except for silk. However, silk is expensive and has a lower stiffness compared to other fibres. The properties of bio-derived fibres suffer from variability, as seen in Table 4. This is because the properties of a bio-derived fibre are dependent on the type of plant, region, type of extraction, fibre age, and processing methods [94]. Apart from variability, the use of bio-derived fibres also possesses challenges such as high moisture absorption, low thermal stability, and poor fire resistance [94,95]. Selection of type of bio-derived reinforcement plays an essential role in achieving adequate performance and overcoming limitations due to the properties variability for any application [94]. Understanding the composition of bio-derived reinforcements and their contribution to the material properties enables the selection of the right type of reinforcement. For example, the properties of natural fibres are governed by the content of

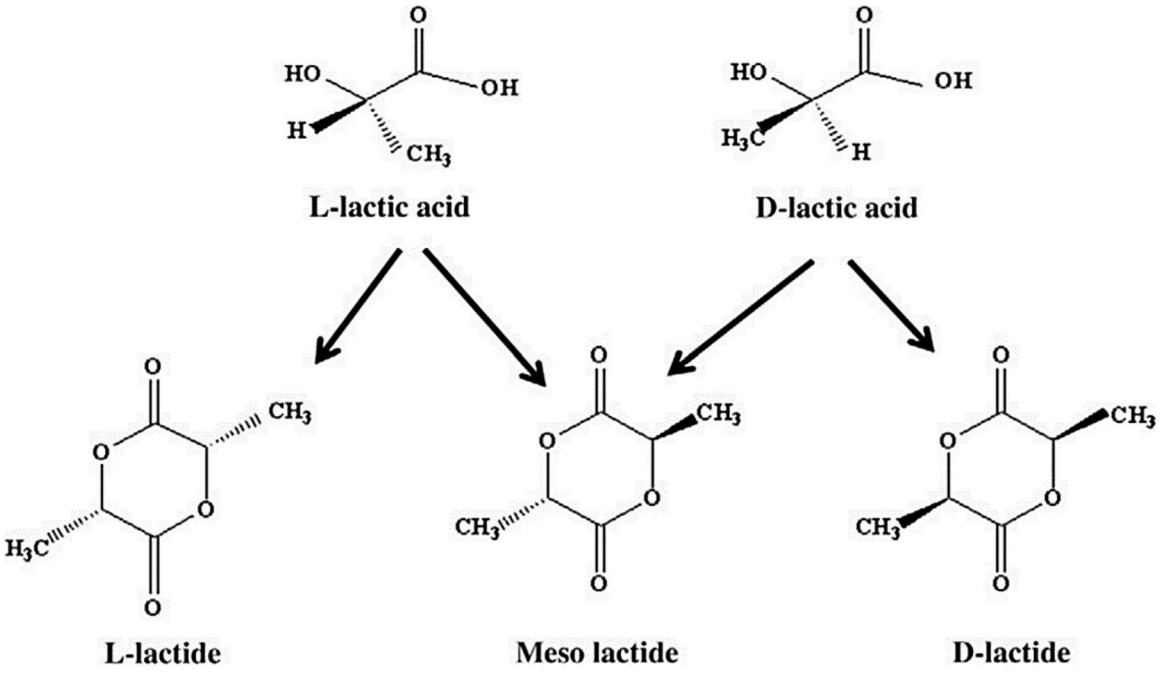


**Figure 10.** Stereoisomers of lactide [85]. Reproduced with permission from Elsevier, license number 5131100470175

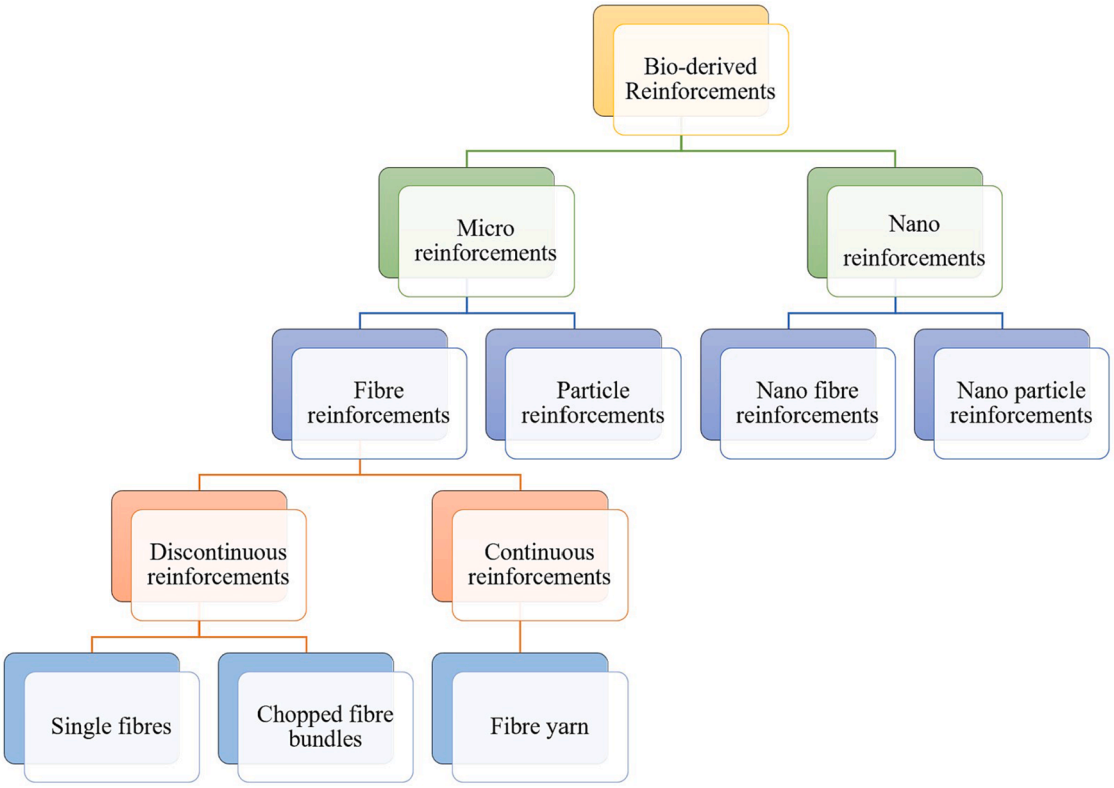


**Figure 11.** Types of bio-derived reinforcements used in FDM composites.

cellulose, micro-fibrillar angle (MFA), and cellulose crystallinity. Lower MFA and high cellulosic content are preferred to achieve high strength and stiffness; however, to achieve high ductility, a higher MFA is preferred [95,96]. In the case of man-made cellulose fibres, the process used to produce the fibres also affects their properties, influencing the degree of crystallinity, micro-void length, and crystal orientation. Man-made fibres produced by the lyocell process, for example, have high crystallinity and lesser void lengths than the fibres produced by viscose and modal processes [97].

Bio-derived reinforcements can also be classified according to their size and shape. For example, bio-derived powder reinforcements include microcrystalline cellulose (MCC), bamboo powder, powdered hemp, and others [64,102–105]. Cellulose nanocrystals (CNCs) and cellulose nanofibres (CNFs) are examples of bio-derived nano reinforcements

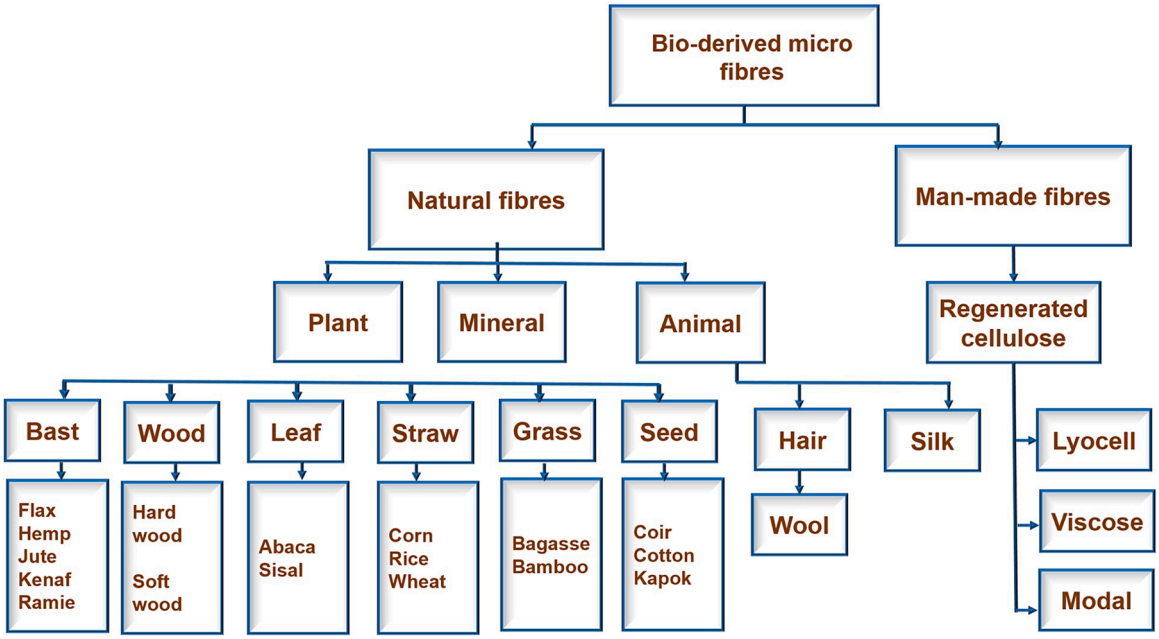


**Figure 12.** Classification of bio-derived micro fibre sources (Adapted from [90]).

**Table 4**
Properties of bio-derived fibres [91,98–101].

| Fibre | Density ($g/cm^3$) | Length (mm) | Tensile strength (MPa) | Young's modulus (GPa) | Failure strain (%) |
|---|---|---|---|---|---|
| Ramie | 1.5 | 900–1200 | 400-938 | 44-128 | 2-3.8 |
| Flax | 1.5 | 5-900 | 345-1830 | 27-80 | 1.2-3.2 |
| Hemp | 1.5 | 5-55 | 550-1110 | 58-70 | 1.6 |
| Jute | 1.3-1.5 | 1.5-120 | 392-800 | 10-55 | 1.5-1.8 |
| Harakeke | 1.3 | 4-5 | 440-990 | 14-33 | 4.2-5.8 |
| Sisal | 1.3-1.5 | 900 | 507-855 | 9.4-28 | 2.0-2.5 |
| Alfa | 1.4 | 350 | 188-308 | 18-25 | 1.5-2.4 |
| Cotton | 1.5-1.6 | 10-60 | 287-800 | 5.5-13 | 3.0-1.0 |
| Coir | 1.2 | 20-150 | 131-200 | 4-6 | 15-30 |
| Curaua | 1.1-1.4 | 1000-1500 | 700-1100 | 30-40 | 3.3-3.9 |
| Silk | 1.3 | Continuous | 100-1500 | 5-25 | 15-60 |
| Feather | 0.9 | 10-30 | 100-203 | 03-10 | 6.9 |
| Wool | 1.3 | 38-152 | 50-315 | 2.3-5 | 13.2-35 |
| Viscose | 1.32 | Continuous | 308-833 | 11-20 | 17-25 |
| Modal | 1.5 | Continuous | 515 - 570 | 14-16 | 11-13.2 |
| Lyocell | 1.5 | Continuous | 552-1019 | 4.7-13.36 | 8-9.4 |

[106,107]. The following sections discuss the production and properties of FDM 3D printed PLA composites with bio-derived reinforcements.

### 4.1. Discontinuous bio-derived micro fibre reinforcements

Biocomposite filaments reinforced with discontinuous natural fibres for FDM are produced by mixing polymers, fibres, and in some cases, additives through melt compounding followed by extrusion. Natural fibres, including hemp, harakeke, bamboo, flax, and others, have been researched for producing PLA biocomposite filaments [88].

Figure 13 compares tensile strength and Young's modulus of discontinuous bio-derived fibre reinforcement/PLA composites manufactured by FDM, injection moulding (IM) and compression moulding (CM). IM and CM are the most commonly used traditional manufacturing methods to produce bio-derived fibre reinforced composites. In compression moulding, the material feedstock is placed in an open heated mould cavity, closed with a top plug, and compressed with a hydraulic press to consolidate the material. Lower cycle time and higher reproducibility are the main advantages of this method [108, 109]. On the other hand, IM involves melting the material feedstock and forcing it into a closed mould to obtain the object of desired shape and dimensions. IM allows for the mass-production of components with high precision economically [110].

The mechanical properties of FDM printed biocomposites are comparatively lower than conventionally manufactured composites [64]. Numerous factors contribute to this, including weak interlayer adhesion, the low fibre content in FDM filaments, the low aspect ratio of bio-derived fibres, and the printed products' porosity [88]. Table 5 summarises the main findings of FDM 3D printed PLA composites with bio-derived discontinuous fibre reinforcements. Values presented in the table are selected based on the composition of reinforcement and PLA that showed the best results in each research work.

Where: FC – fibre content.

Fibre content has shown to have the highest effect on the mechanical properties of discontinuous fibre reinforced composites. Tensile strength of FDM printed PLA biocomposites has been observed to increase with an increase in fibre content, but composites with fibre contents higher than 20 wt% are usually highly viscous, making extrusion non-uniform and causing clogging of the extruder die or printer nozzle [76,77]. For example, by using 20 wt% harakeke fibres as reinforcement for PLA, an increase of 42.5% and 5.4% in Young's modulus and tensile strength, respectively, were achieved compared to neat PLA. However, increasing fibre wt% above 20% caused uneven surface and poor interlayer adhesion. Fibre pull-out was observed in fractured samples showing weak fibre/matrix adhesion [111].

It has also been observed that porosity in a 3D printed sample increases with the increase in fibre content. Some of the proposed solutions to decrease porosity in 3D printed biocomposites include vacuum drying of the fibres, controlling humidity and temperature throughout the printing process, and the use of plasticisers [116,125]. Applying vacuum at the end of extrusion and adequate drying of the composite filaments has resulted in reduced porosity in FDM printed PLA composites reinforced with discontinuous flax and bamboo fibres [116]. For example, PLA was compounded with two types of plasticisers (provided by Proviron Industries NV) and then reinforced with bamboo and flax fibres individually. A vacuum pump was used at the end of the compounding line to reduce porosity, and 3D printing filaments with up to 4% voids were produced. It was observed that high extrusion speeds resulted in filaments with smoother surfaces. The highest improvement

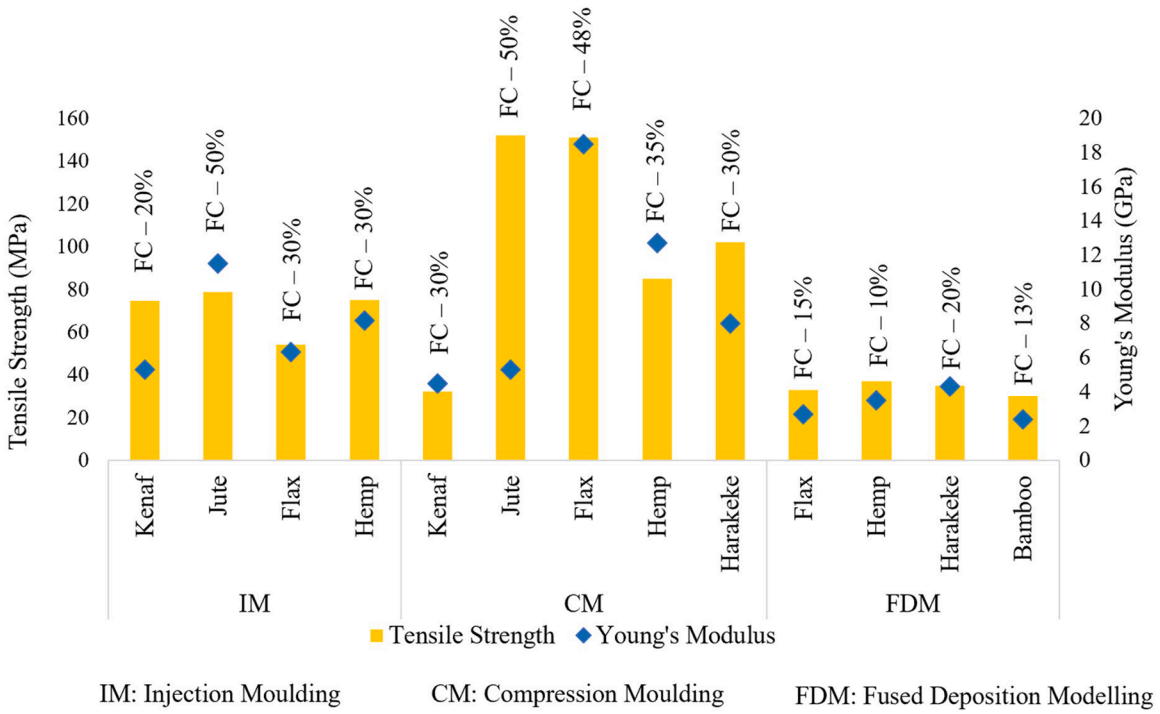


**Figure 13.** Tensile strength vs Young's modulus of discontinuous bio-derived fibre reinforcement/PLA composites [46,72,8,73–77,78,117–121,111,116,122].

**Table 5**
Summary of main findings of FDM 3D printed PLA composites with bio-derived discontinuous fibre reinforcements.

| Reinforcement | Reinforcement content (wt %) | Modification/treatments | Characterisation specimen type | Tensile strength (MPa) | Young's modulus (GPa) | Observations | Ref. |
|---|---|---|---|---|---|---|---|
| Hemp | 10 | Alkali fibre treatment with 5% NaOH | Printed sample | 37 | 3.5 | Improvement in tensile properties was observed. The use of plasticiser was suggested to improve interlayer adhesion and surface quality. | [111] |
| Harakeke | 20 | Alkali fibre treatment with 5% NaOH+ 2% sodium sulphite | Printed sample | 36 | 4.2 | 3D printed PLA/harakeke composite demonstrated a 42.3% and 5.4% increase in Young's modulus and tensile strength, respectively, compared to neat PLA. | [111] |
| Flax | 15 | PLA was compounded with two types of plasticizers sourced from Proviron Industries NV, whose types were not mentioned by the authors. | Filament (ASTM D3039 standard) | 33 | 2.7 | Filaments with only up to 4% voids were produced. | [116] |
| Bamboo fibre (BF) | 13 | PLA was compounded with two types of plasticizers sourced from Proviron Industries NV (Belgium) | Filament (ASTM D3039 standard) | 30 | 2.4 | L/d ratio of bamboo fibres had a direct effect on Young's modulus. BFs with a length of 2.14mm displayed an improvement of 215% in Young's modulus compared to neat PLA. | [116] |
| Sugar cane bagasse fibre (SCBF) | 6 | Raw sugarcane bagasse was treated with 7.5-wt% NaOH solution to obtain SCBF | Printed sample (ISO 527 standard) | 57.1 | - | The highest mechanical properties were observed for the samples printed in the parallel direction to the build plate. SCBF was observed to promote the crystallisation of PLA. | [122] |

in Young's modulus was recorded for bamboo fibres with a 230% improvement compared to PLA compounded with a plasticiser. Although the aspect ratio of flax fibres was higher than bamboo fibres, a higher increase in stiffness was not observed due to loss of orientation in the compounding process [116].

### 4.2. *Continuous bio-derived micro fibre reinforcements*

Using continuous natural fibre reinforcements could provide an opportunity to achieve higher mechanical properties. Most commercially available FDM 3D printing filaments with continuous reinforcements use continuous carbon fibre and kevlar fibre. Recently, researchers have developed customised methods to produce composite filaments with continuous natural fibre reinforcements [126–129]. Studies show that composites with continuous reinforcements, such as jute/PLA, and flax/PLA, have exceeded the mechanical properties of composites with discontinuous reinforcements [88]. FDM 3D printers used to fabricate composites with continuous reinforcements are modified to include two material supplies – the thermoplastic polymer and the continuous fibre. Examples of two different printers with single and dual nozzle systems are shown in Figure 14. In a single nozzle printer (see Figure 14 (a)), thermoplastic polymer and continuous reinforcement are passed

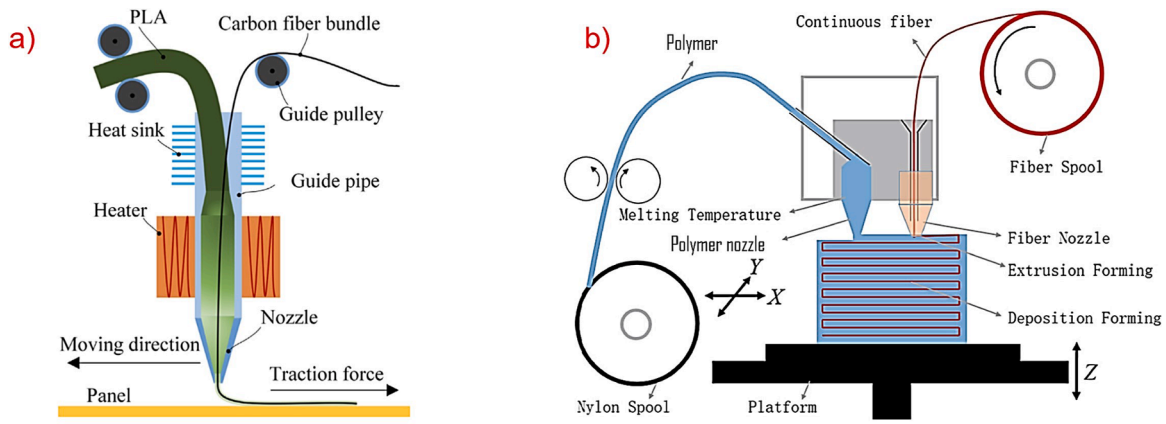


**Figure 14.** FDM 3D printing process for continuous fibre composites with a) single nozzle [131] Reproduced with permission from Elsevier, license number 5170290431014 b) dual nozzle Reproduced with permission from Elsevier, license number 5124221090291 [132].

through the heated nozzle. The temperature of the nozzle is set according to the melting temperature of the thermoplastic matrix. The matrix and fibre fuse together and are deposited layer by layer [130].

Figure 14 (b) shows the working mechanism of the dual nozzle printer. This printer uses two different nozzles to deposit the matrix and continuous fibres separately. One nozzle stops while the other is moving, and the continuous reinforcement is sized to the thermoplastic polymer to adhere to the previous layer. This dual nozzle printer allows customised fabrication and minimises cost [133]. So far, studies involving PLA/continuous natural fibre reinforcements have mostly used single nozzle type FDM printers [134,135]. Some studies also involved direct FDM 3D printing of PLA coated natural fibre yarns [127,136].

Results from current studies show the potential for achieving mechanical properties of 3D printed continuous natural fibre reinforcement/PLA composites comparable to that of continuous carbon fibre/PLA composites [137]. Reinforcement type, fibre content, production method, and tensile properties of 3D printed PLA composites reinforced with continuous bio-derived fibres are summarised in Table 6.

The selection of fibre, the volume fraction of the fibre, and fibre/matrix interfacial adhesion play a critical role in achieving desired mechanical properties. For example, the highest tensile properties were achieved by flax/PLA composites and were attributed to the higher strength of the flax fibres, the higher aspect ratio of the flax fibre (L/d <10), higher fibre volume fraction (30.4%), and lower porosity content ($v_p = 3.2 \pm 0.7\%$) [138].

It is essential to optimise processing parameters to produce continuously reinforced PLA 3D printed composites with maximum interfacial adhesion to avoid failure due to defects. Figure 15 shows SEM images of longitudinal and transverse fracture surfaces of 3D printed flax yarn reinforced PLA composites. The failure behaviour observed from tensile tests and SEM showed a quasi-linear section associated with flax/PLA interface debonding followed by debonding of flax fibre bundles within the yarn. Highlighted areas in Figures 15 (a) and (b) show brittle, quasi-linear stress-strain behaviour associated with a smooth surface and debonding of significant lengths of fibres. This shows that the flax yarn had weak cohesion because of the highly twisted structure and incomplete impregnation of PLA into the flax fibre [138]. Due to poor interfacial adhesion, a similar pull-out of fibres was observed in jute yarn/PLA FDM 3D printed composites. This was attributed to incomplete wetting of jute yarn by PLA, and fibre surface treatment was suggested to improve the fibre/matrix adhesion [134].

The importance of interfacial adhesion with respect to tensile properties of continuously reinforced PLA/flax composites has been demonstrated at the 3D printing filament production level. Flax yarn was coated with PLA to obtain continuously reinforced FDM filaments of different diameters. An increase in tensile strength with a decrease in filament diameter was observed, confirming higher tensile strength for composite filaments with higher flax content. However, this trend was not displayed for 0.8 mm filament as the tensile strength was lower than 1mm filament despite having a higher flax content due to insufficient adhesion of flax and PLA, as shown in Figure 16. The non-uniform coating at lower filament diameters is due to the limitations of the filament production process pertaining to the extruder geometry. Since the extruder die was placed vertically and the upper hole had a diameter of 1.2 mm, the chances of air bubbles entering were high, which caused the roughness in the surface of filaments [127].

Future possibilities to improve the mechanical performance of continuous bio-derived reinforcements/PLA composites include developing customised filament production methods, optimising printing parameters, using low twist yarns, and exploring more reinforcement options [88].

### 4.3. *Particulate reinforcements*

Bio-derived particle reinforcements in composites provide less reinforcement than fibres and are generally used in polymer matrices to improve Young's modulus [140]. Most commercially available PLA FDM filaments with bio-derived particles are based on wood powder [141,142]. Although many bio-derived particles have been extensively studied for 3D printability [140,143,152,144–151], only a few materials, including MCCs, hemp powder, and bamboo powder, have displayed a reinforcing effect when combined with PLA for FDM 3D printing, as shown in Table 7. Values presented in the table are selected based on the composition of reinforcement and PLA that showed the best results in each research work.

Bio-derived particle reinforced 3D printing filaments are produced by compounding PLA with particle reinforcements by batch mixing with twin-screw extruders. For extrusion, filament diameter and dimensional tolerances play a significant role in determining the particle size [154,155]. Most benchtop FDM printers require mechanical refining or ball milling of reinforcements to avoid nozzle clogging during extrusion. The most commonly used particles are wood flour produced by ball milling and microcrystalline cellulose. PLA and bio-derived particles need to meet the requirement of less than 0.1% moisture content to avoid the reaction of PLA with water at high temperatures, which excises chains and reduces the properties of the 3D printed composite [150]. An increase in particle content leads to inconsistent flow and variation in diameter and reduces the mechanical properties of the filament. An example of the formation of voids and pores with increasing particle content can be seen in Figure 17 [153]. Various approaches to overcome these issues and improve the properties of PLA reinforced with bio-derived materials will be discussed in further sections.

**Table 6**
Production and properties of FDM 3D printed PLA/continuous bio-derived fibre reinforced composites.

| Reinforcement | Fibre Content | Production of composite filament and 3D printing | Tensile Strength (MPa) | Young's modulus (GPa) | Ref. |
|---|---|---|---|---|---|
| Flax fibre yarn | 20.4 wt% for maximum tensile strength, 36.7 wt% for maximum Young's modulus | Molten PLA was squeezed through the crosshead extrusion die of a single-screw extruder. Flax yarn was introduced through the vertical opening of the die and coated with PLA. The filament was collected, and a five-axis FDM 3D printer was then used to print with the composite filaments. | 89 | 2.9 | [127] |
| Flax fibre yarn | 30.4 wt% | Flax yarn was coated with PLA using a single screw extruder. Flax yarn of 68 tex was used, and the extrusion temperature was set to 180°C. FDM printer modified to incorporate a custom 1.8mm nozzle was used for 3D printing. | 254 | 23 | [138] |
| Pineapple leaf fibre yarn | - | A single nozzle type 3D printer was used. The pineapple leaf fibre yarn and the PLA filament were blended in the extruder with a 1:4 volume fraction and were consolidated at the hot end to form a composite. The composite filament was extruded through the nozzle in a layer-by-layer fashion to form a 3D printed part. | 96.8 | - | [135] |
| Jute fibre yarn | 6.1% volume fraction ($V_f$) | A single nozzle type continuous fibre 3D printer was developed where PLA filament was supplied using drive gears and a stepping motor, and the jute yarn was supplied to the printer head automatically by the movement of the PLA filament. The PLA filament melts inside the printer head, merging the yarn and PLA in the heated segment. The composite filament is extruded onto the hot plate in a layer-by-layer pattern. | 57.1 | 5.11 | [134] |
| Ramie fibre yarn | | A single nozzle type 3D printer, Combot-200, was used to fabric PLA/ramie composites using an in-situ impregnation method. | 86.4 | 0.6 | [139] |

### 4.4. Nano reinforcements

Bio-derived nano reinforcements used in FDM 3D printing PLA are all different types of nano celluloses and are categorised into cellulose nanocrystals (CNCs), nano fibrillated cellulose (NFC), and bacterial nanocellulose (BC) [156]. Nano celluloses have low density, ultra-fine structure, and high mechanical properties, making them potential candidates for reinforcement of thermoplastics. CNC is obtained from acid hydrolysis of cellulose and contains 100% cellulose, and its shape is rod-like with a diameter of 2-20nm and a length of 100-500nm. NFC, also known as cellulose nanofibril (CNF), can be obtained by mechanically refining cellulose fibrils and has a composition of 100% cellulose with both amorphous and crystalline regions. NFC has a square cross-section with a 1-100nm diameter and a length of 500-2000nm [157]. Bacterial cellulose is obtained from microfibrils secreted from various bacteria separated from bacterial bodies and growth mediums. The morphology of BCs depends on their sources, and they usually have a square or rectangular cross-section. For example, Acetobacter microfibrils have a rectangular cross-section of 6–10 nm by 30–50 nm [92].

Table 8 summarises the main findings in FDM 3D printed PLA composites reinforced with CNCs, NFC, and BC. Values presented in the table are selected based on the composition of reinforcement and PLA that showed the best results in each research work.

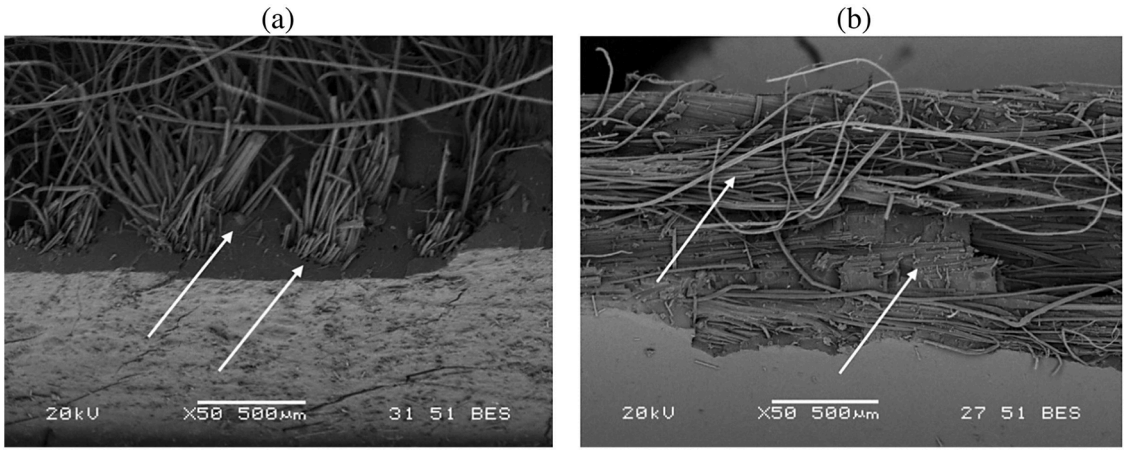


**Figure 15.** SEM images of fracture surfaces of FDM 3D printed flax yarn/PLA 3D printed composites (a) longitudinal, transverse fracture (b) transverse fracture [138].

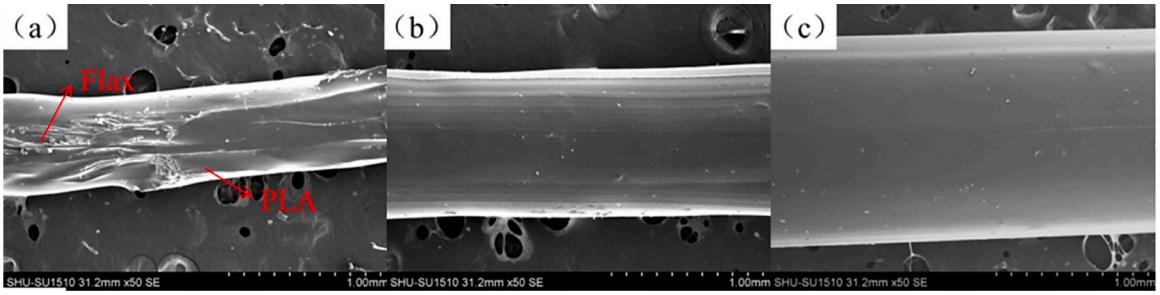


**Figure 16.** SEM images of the flax yarn/PLA composite filaments with diameters of 0.8 mm (a), 1.0 mm (b), and 1.2 mm (c) [127].

**Table 7**
Summary of main findings of FDM 3D printed PLA composites with bio-derived particle reinforcements.

| Reinforcement | Reinforcement content | Modification/ treatments | Tensile strength (MPa) | Young's modulus (GPa) | Elongation at break (%) | Observations | Ref. |
|---|---|---|---|---|---|---|---|
| Hemp powder | 5wt% Hemp | Untreated | - | 3.1 | - | An increase in storage modulus with an increase in hemp volume fraction was observed. Only composites with 5 wt % Hemp displayed better storage modulus than neat PLA. | [103] |
| Bamboo powder (BP) | 20wt% BP | The bamboo powder was treated with $CaCO_3$ | 51 | - | - | $CaCO_3$ treated BP composites demonstrated the best results with an increase of 40.33% in tensile strength. | [105] |
| MCC | 5wt% MCC | Joncryl® ADR-4368C used as an epoxy-based chain extender | 45 | 3.2 | - | Improvement in mechanical properties. Lower density samples due to the presence of voids. | [102] |

One of the main challenges in using nano cellulose as reinforcement in PLA is that the hydrophilic cellulose has a tendency to aggregate in the hydrophobic PLA matrix, and thus chemical/physical treatments have been used to improve dispersion [164]. Esterification/acetylation, silylation, TEMPO mediated oxidation, and grafting of molecules or macromolecular groups to nanocellulose are the widely used approaches for surface modification of nanocellulose [165].

CNFs have been grafted with L-lactide monomer to form PLA grafted CNFs (PLA-g-CNFs). A post extrusion annealing treatment was performed on the FDM filaments, which resulted in a 66% increase in tensile strength and 28% in stiffness with 3% of PLA- g-CNF [158]. The Pickering emulsion method was used to add TEMPO (2,2,6,6-Tetramethylpiperidin-1-yloxy) oxidised bacterial cellulose (BC) to PLA, resulting in an improvement in the dispersion of nanocellulose in the PLA matrix and enhanced mechanical properties [161].

In all the FDM 3D printing studies done so far, the best mechanical properties have been achieved for 30wt% CNF reinforced composites. To avoid agglomeration of CNFs at high loadings, chopped and freeze-dried CNF networks that act as microsponges were used that allowed PLA to flow into them during melt processing by creating mechanical interlocking. The high interfacial adhesion between CNFs and PLA was attributed to the low packing density of CNFs combined with the low viscosity of PLA in the molten state [162].

Figure 18 shows fracture mechanisms in CNC and CNF composites before, during, and after mechanical stress. The dimensions and shape of the reinforcement material affect the microstructure of the composite. CNCs have a spherical/oblong shape, due to which their lengths are shorter in comparison to the fibril shape of CNFs, which allows them a higher chance of diffusion. CNFs also tend to have better reinforcement than CNCs efficiency because of their higher aspect ratio. CNFs have an aspect ratio of 25-500 compared to 10-100 for CNCs [166]. CNF composites have displayed a higher number of bridging nanofibrils on the

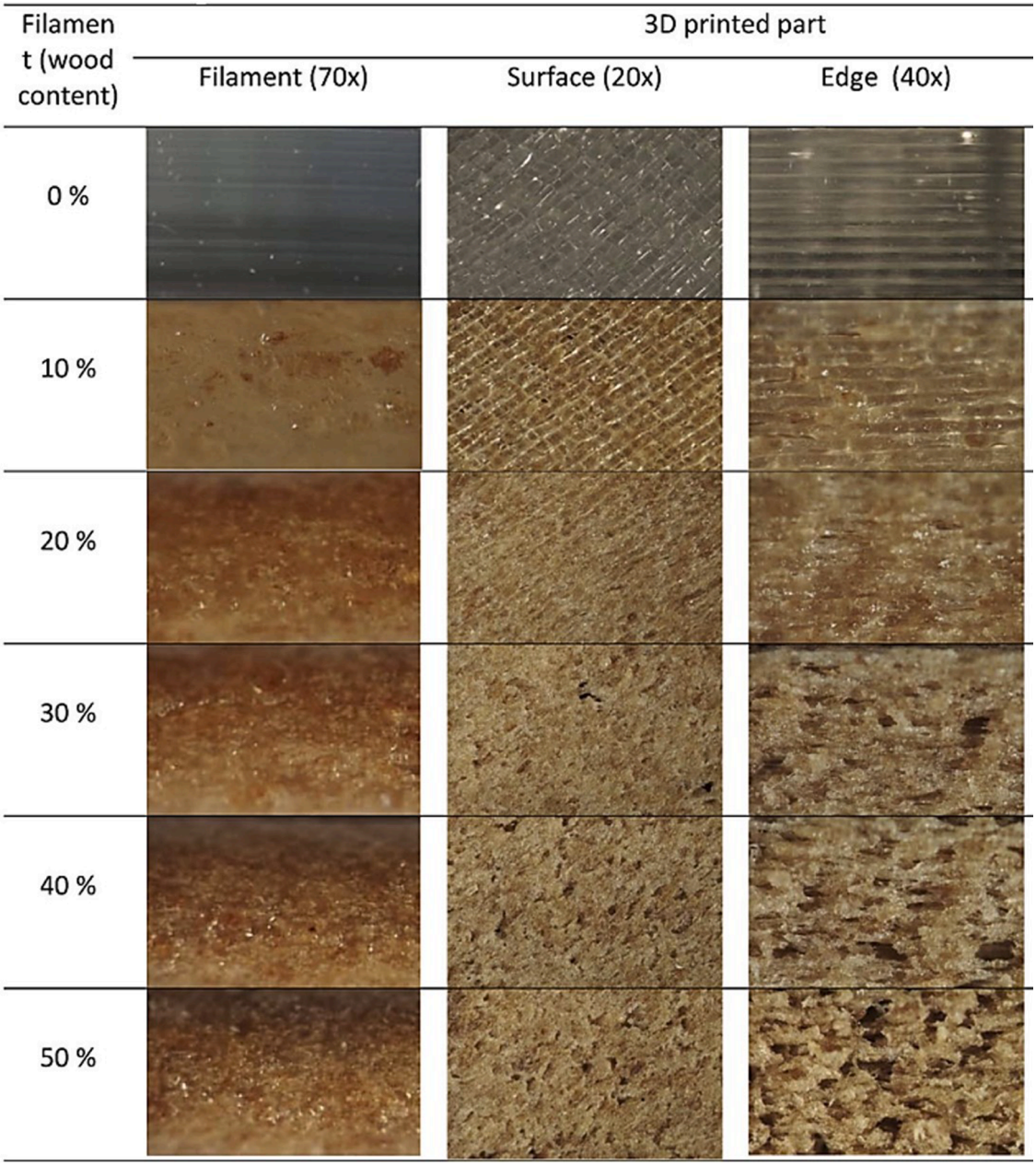


**Figure 17.** Optical micrographs of wood/PLA filament(left), surface (middle), and edge (right) [153]. Reproduced with permission from Elsevier, license number 5167000723403.

fracture surface than CNC composites. Each nanofibril can bridge a crack at multiple locations leading to better stress distribution and stronger composites [167].

### 4.5. Enhancing properties of FDM 3D printed PLA biocomposites

Overall enhancement of properties of FDM 3D printed biocomposites can be achieved by introducing modifications at three different stages. The first stage is before 3D printing, where modifications can be introduced on a material level that helps improve interfacial bonding between PLA and bio-derived reinforcements. The second stage is 3D printing, where optimising printing parameters can help achieve efficient printing and improved properties. The third stage is post 3D printing, where enhancement of properties is achieved by reducing defects using post-processing methods. A detailed overview of processes followed for these three different stages to enhance FDM 3D printed PLA properties are presented here.

*Pre-3D Printing Stage*

PLA used for FDM is semi-crystalline and molecular chains of PLA exhibit imperfect molecular symmetry, affecting the diffusion ability and crystallinity of PLA, mainly within the limited window of time in the FDM printing, leading to low mechanical properties and weak bonding between the printed layers [153–157]. Studies show that adding plasticiser such as polyethylene glycol (PEG) improved the crystallinity and mechanical properties of PLA. On the other hand, more than 10 wt% of PEG was shown to depreciate PLA properties as a PEG crystallisation peak occurred in DSC, which shows the separate existence of PEG [168–170]. As mentioned earlier, the addition of plasticisers also helped in decreasing the porosity of FDM 3D printed PLA composites [116].

Cross-linking degree of molecular chains of PLA was improved by adding synthetic low molecular weight (LMW) PLA components to

**Table 8**
Summary of main findings of FDM 3D printed PLA composites with bio-derived nano reinforcements.

| Materials | Reinforcement content | Modifications/treatments | Tensile strength (MPa) | Young's modulus (GPa) | Elongation at break (%) | Observations | Ref. |
|---|---|---|---|---|---|---|---|
| CNF | 2.5 wt.% | PEG600 was used as a plasticizer. To obtain CNF, enzymatic hydrolysis of MCC was performed. | 57.5 | - | 8.5 | CNF filled PLA biocomposite filament showed an increase of 33% in tensile strength and 19% in elongation at break. | [112] |
| CNF | 3 wt% | PLA grafted CNFs (PLA-g-CNF) were obtained by grafting L-lactide monomers onto CNFs | 45.2 | 3.5 | - | Tensile testing of filaments showed 66% increase in tensile strength and 28% in stiffness. | [158] |
| Nanocellulose | 1 wt% | Nanocellulose was obtained by ultra-sonication of micro cellulose | 41.5 | 2.6 | 5.5 | Tensile tests showed the highest improvement in the stiffness and stress at the break with 1% nano cellulose in PLA. | [159] |
| PHB/ CNC | 1wt% | Dicumyl peroxide (DCP) is used as a cross-linking agent | - | - | - | Improvement in interfacial adhesion and thermal stability. | [160] |
| TEMPO-oxidized BC - (TOBC) | 1.5wt% | BC was subjected to a TEMPO mediated oxidation | 32 | 3.7 | - | Improvement in crystallinity, mechanical strength, and toughness. | [161] |
| CNF | 30wt% | Untreated | 80 | 7.1 | 1.5 | Improvement in tensile strength and young's modulus by 45% and 130%, respectively. A decrease in elongation and toughness was observed. Significant improvement in storage modulus was achieved. | [162] |
| Sisal CNF | 1 wt% | Untreated | 52.14 | 3.7 | 2.39 | Tensile strength and Young's modulus increased by 84% and 63%, respectively, with 1wt% CNF. Adding CNF also improved crystallisation and decreased voids. | [163] |

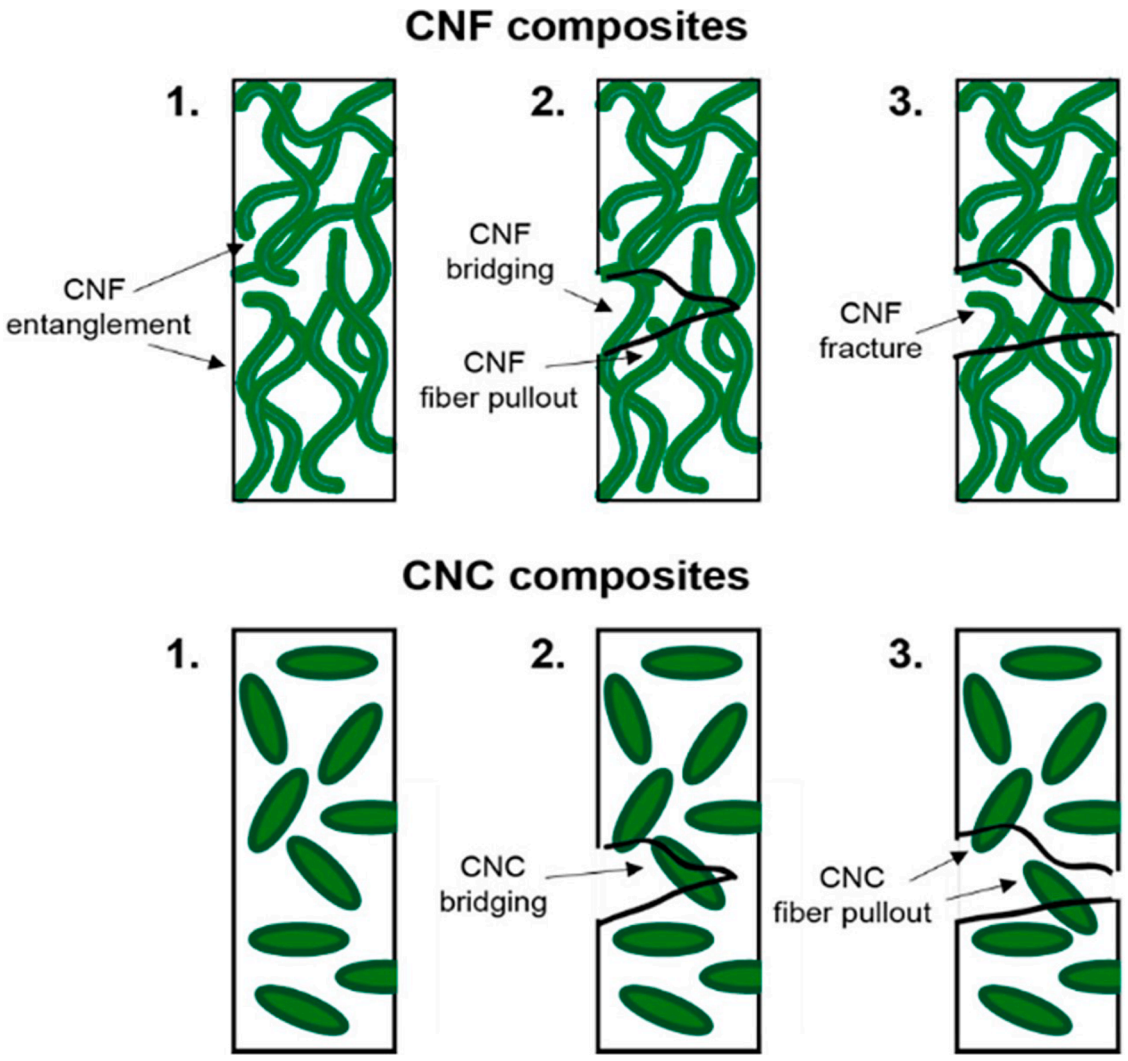


**Figure 18.** Fracture mechanisms in CNC and CNF composites 1) before mechanical stress 2) during mechanical stress 3) after mechanical stress [166].

commercial PLA. It was observed that LMW PLA diffuses more quickly across the inter-filament interface during the deposition of layers improving the interlayer bond [171]. However, filaments extruded through the nozzle during the FDM process stay in the molecular diffusion and crystallisation temperature for a short time. To overcome this issue, researchers have added radiation-sensitive materials to PLA filaments before 3D printing and then irradiated the printed parts by electron beam, γ-ray, or microwave. Upon irradiation, free radicals are generated in the primary or side chain of PLA, allowing further cross-linking [60]. Similarly, in another experiment, PLA was blended with γ-ray sensitive trimethylolpropane triacrylate (TMPTA) and trially isocyanurate (TAIC) and 3D printed by FDM. The 3D printed part was then radiated by γ-ray, and the temperature was set to near $T_g$. This experiment showed an improvement in the tensile properties of radiated PLA compared to the non-radiated one [172].

Interfacial shear strength (IFSS) directly affects the efficiency of load transfer between fibre and matrix, thereby determining the mechanical performance of discontinuous fibre reinforced composites [64,92, 173–176]. IFSS is defined as the product of the dynamic coefficient of friction and the clamping residual stress. IFSS is used to determine the stress required for fibre sliding in fibre-reinforced composites. It is one of the key interfacial properties and represents the strength required to overcome the chemical bonding between the fibre and matrix. In the absence of any chemical bonding between the fibre and the matrix material, IFSS represents the amount of strength required to overcome the static coefficient of friction between the fibre and the matrix [177].

One of the main challenges to achieving good interfacial bonding is creating surface-chemical compatibility between the hydrophilic bio-derived reinforcements and the hydrophobic PLA matrix [178,179]. Several physical, chemical, and biological treatments have been proposed to reduce the hydrophilicity of the reinforcement surface and improve reinforcement/matrix adhesion [46]. Surface modification and compatibilisation of the matrix are the most used methods to improve interfacial adhesion [178]. Tables 9 and 10 summarise recent research on surface modification and PLA matrix compatibilisation, respectively.

### 3D. Printing Stage

Various factors, including build orientation, printing temperature, and raster angle, affect the mechanical properties of a 3D printed polymer composite [61]. However, studies on the influence of printing parameters on the properties of FDM printed PLA biocomposites are limited and have only recently been reported [193]. Higher extrusion temperatures have been shown to improve adhesion between matrix and fibre and improve tensile properties. 3D printing PLA/PHA wood filaments and PLA/hemp filaments by increasing printing temperatures from 210°C to 230°C resulted in an improvement in tensile strength. However, increasing the printing temperature above 230°C led to a decline in tensile properties due to thermal degradation of bio-derived fibres [152,194]. Partial thermal degradation of bio-derived fibres was correlated with the reduction in thermal stability decomposition of hemicellulose and lignin, which occurs between 210°C to 370°C. Hemp fibres, for example, have been concluded to be thermally stable in the range of 110°C to 210°C [194]. Flax fibres, on the other hand, displayed thermal degradation after 220°C [195]. Reduction in tensile properties at high temperatures was also associated with the accumulation of filament at the extruder nozzle causing defects in the filament.

Effects of printing orientation on PLA/sugarcane bagasse fibre (SCBF) composites were studied, and it was found that longitudinal orientation (0°) displayed the best tensile properties with a tensile strength of 57.1 MPa compared to 42.6 MPa in vertical (90°) direction [122]. However, in another research, PLA/agave fibre composites were studied to understand the effect of raster angle. It was found that tensile and flexural properties were not impacted significantly by the raster angle, and impact strength slightly increased at -45°/45° [196].

Along with printing parameters, interlayer adhesion of deposited filaments also significantly impacts the mechanical properties of FDM 3D printed PLA parts. The main reason for weak interlayer bonding is that PLA cannot maintain enough time at melting temperature. In the FDM process, the temperature of PLA drops quickly after the filament is extruded. As a result, molecular chains on the interface of PLA are not diffused completely, and these filaments cannot be fused with the newly extruded filaments effectively. This effect results in anisotropic material behaviour and reduced strength caused by voids formed during printing [197].

The cooling rate parameter plays a crucial role to improve interlayer bonding. If the cooling speed is too slow, resulting PLA parts have poor surface quality and may also result in deformed shapes. If the cooling speed is too high, molecular diffusion on the surface decreases, and the interface bond between layers becomes weak [198]. Researchers have

**Table 9**
Recent works involving surface modification to improve interfacial adhesion in PLA composites with bio-derived reinforcements.

| Composite | Modifier | Effects on composite properties | Ref. |
|---|---|---|---|
| PLA/Unidirectional Flax fibres | Lignin and Tannin | Tannin showed better results. A 17% and 29% increase in ultimate flexural strength and interlaminar shear strength, respectively, was observed. | [180] |
| PLA/Coir fibres/ Pineapple leaf fibres | Alkali treatment with 6% NaOH solution | Improvement of 128% and 112% was observed in tensile strength and Young's modulus, respectively. | [181] |
| PLA/ Poplar Fibre | Maleic Anhydride and KH550 | Tensile strength for 0.5% MA and 2% KH550 improved by 17% and 23%, respectively. | [182] |
| PLA/ Kenaf/ Montmorillonite (MMT) clay | Kenaf fibres were treated with 6% NaOH solution | Increase in impact, flexural and tensile strengths by 11%, 46% and 6%, respectively. | [183] |
| PLA/ Pineapple leaf fibre yarn PLA/ sisal fibre yarn | Alkali treatment with 5 wt% NaOH solution | Improvement in thermal stability and tensile properties. | [184] |
| PLA/Bacterial cellulose (BC) | BC was subjected to a TEMPO mediated oxidation | Improvement in crystallinity, mechanical strength, and toughness. | [161] |
| PLA/CNF | CNFs were grafted with L-lactide monomer to form PLA grafted CNFs (PLA-g-CNFs) | 66% increase in tensile strength and 28% in stiffness with 3% of PLA- g-CNF | [158] |
| PLA/CNF | CNFs were grafted with L-lactide monomer to form PLA-g-CNFs | Increase in tensile strength, Young's modulus, elongation at break, and impact strength by 20%, 31.8%, 12%, and 27.9%, respectively, compared to PLA/CNF composite. | [185] |
| PLA/CNC | Immobilised Lipase was used to catalyse the formation of laurate ester groups on the CNC surface | 66% increase in tensile strength, 61% increase in elongation at break, and improvement in crystallinity. | [186] |
| PLA/CNC | Acetic anhydride was used for surface modification of CNC. Dropwise acetylation was performed by using 3g CNC, 4.5g pyridine, and 114g acetic anhydride | Improvement in barrier properties, interfacial compatibility, and mechanical properties. | [187] |

**Table 10**
Recent works involving matrix compatibilisation to improve interfacial adhesion in PLA composites with bio-derived reinforcements.

| Composite | Compatibilizer | Effects on composite properties | Ref. |
|---|---|---|---|
| PLA/Lemongrass fibre (LF) | PLA grafted with maleic anhydride (PLA-g-MAH) | Improvement of tensile strength, impact strength, and flexural strength. | [188] |
| PLA/ Microcrystalline cellulose (MCC) | Maleic anhydride-grafted PLA (PLA-g-AMS/MAH) | The compatibilisation effect was seen to increase with an increase in $D_g$ (grafting degree) of PLA-g-AMS/MAH. | [189] |
| PLA/ Tannin | Methylene diphenyl diisocyanate(p-MDI) | An increase in the tensile strength of the composite by 19.1% was recorded. Moreover, there was an improvement in melting temperature and thermal degradation onset temperature. | [190] |
| PLA/Sisal PLA/Flax | Maleic anhydride-modified PLA (MA-PLA) | Improvement in tensile strength was achieved. In comparison, the tensile properties of flax fibre composites were superior to sisal fibre composites. | [191] |
| PLA/ Wood fibres | Maleic anhydride-modified PLA | Good interfacial adhesion at higher wood fibre loadings (up to 80%). | [192] |

studied and implemented heating of the pre-deposition layer as a solution to resolve the anisotropy problem caused by interface bonding between layers in FDM printed PLA parts [199].

A synchronous and local laser heating system was proposed to heat the layered zone of PLA near the nozzle, as shown in Figure 19. The temperature at the interface was raised to exceed the $T_g$. Results showed that interface diffusion of PLA molecules increased, improving the interface bond between layers. More than 60% improvement in strength and 100% improvement in elasticity were recorded [199,200]. A similar method was employed using an infrared lamp to increase the temperature at the interface of PLA layers. As shown in Figure 20 (a), three different experimental conditions were set. A comparison of average mechanical properties is shown in Figure 20 (b). Conditions 1 and 2 show a significant improvement in fracture energy, whereas condition 3 shows a decline in properties. This was explained by the use of infrared radiation of 1 kW, which led to the degradation of the mechanical properties of PLA [201].

The local laser pre-deposition heating and infrared preheating use external heating sources to control the local printing temperature, which improves the interface bonding of printed layers. This results in improved mechanical properties of FDM 3D printed PLA as there are low residual stresses during controlled cooling. However, it is essential to consider cost and complexity factors while employing these technologies for FDM.

*Post 3D Printing Stage*

Defects in 3D printed natural fibre reinforced PLA composites that affect the mechanical strength are due to residual stresses, uneven fibre distribution, and poor bonding between fibre and matrix [88]. Residual stresses caused due to 3D printing process and changes in the crystal structure of PLA are interrelated. PLA exhibits four different crystalline forms, namely α, β, γ, and δ. The most common form is the α form that is obtained from a slow cooling procedure from a melt solution. β form is obtained from the deformation of α form by drawing PLA at high temperatures. γ form of PLA is a result of epitaxial crystallization on a single substrate like hexamethylbenzene. The δ form (or α' form) has a similar crystal structure to the α form and is obtained upon fast cooling from a melt [202–205]. The δ form occurs during the fast cooling process while 3D printing and is metastable. PLA has thermal and mechanical stability in this form [202]. Annealing is used as a post-processing method to reduce residual stress and increase the crystallinity of FDM printed PLA components. Annealing is a process where the material is reheated and held above or near its $T_g$ and then allowed to cool slowly. This heating and prolonged cooling remove the δ form, redistribute the stresses, and increase the crystallinity resulting in improved strength and stiffness [206,207]. Annealing at 120°C for 10 minutes showed to improve crystallinity and reduce residual stresses [202]. Another study showed that the best results in improved tensile strength were obtained when PLA was annealed at 80°C. However, annealing also causes deformation leading to changes in the dimensions of the PLA parts depending on the grade of PLA used. To achieve accurate dimensions, deformation is a significant factor to be considered [208].

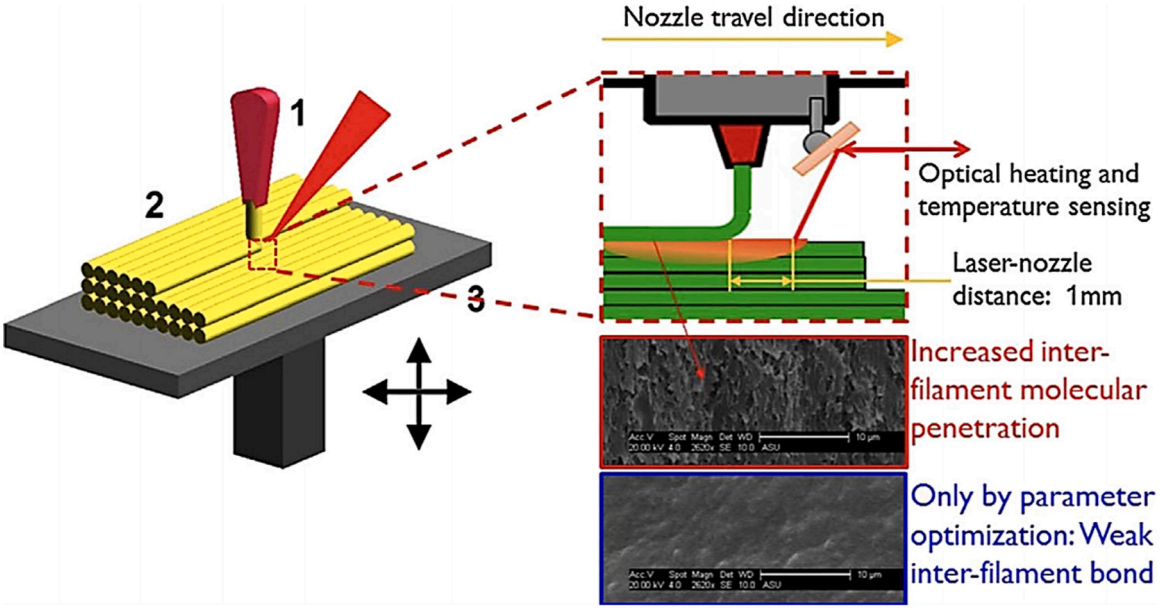


**Figure 19.** Concept diagram of laser local pre-deposition heating method to improve interface bond of PLA layers in FDM 3D printing [200]. Reproduced with permission from Elsevier, license number 5124230169886.

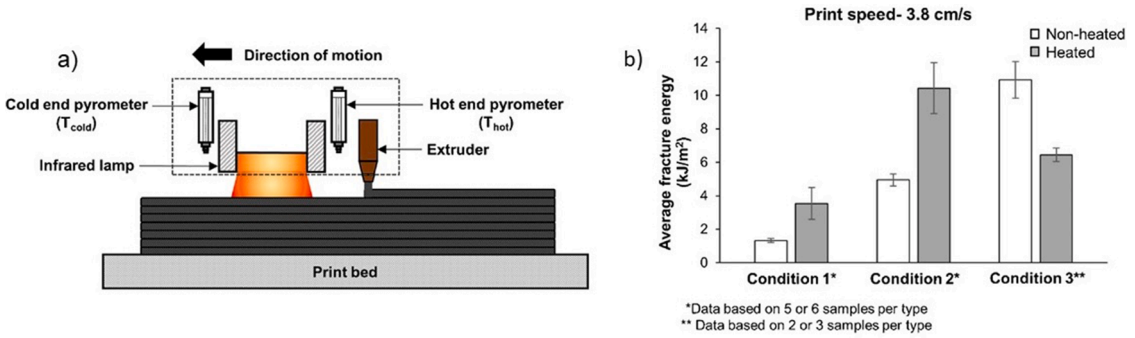


**Figure 20.** a) Infrared preheating experimental setup b) variation of fracture energy for various preheating conditions [201]. Reproduced with permission from Elsevier, license number 5124230347232.

## 5. FDM 4D Printing of PLA and its Bio-Derived Composites

As stated earlier, PLA exhibits shape-memory behaviour as a response to a thermal stimulus. Figure 21 shows a complete cycle of shape-memory mechanism in PLA consisting of the original programmed shape, deformed temporary shape, and recovered original shape. Shape-memory systems based on PLA are often programmed at temperatures above their $T_g$ and further cooled to have a fixed temporary shape. The original shape of the material is recovered upon raising the temperature above its $T_g$. At a microscopic level, shape recovery is triggered by the polymer chain mobility induced by glass transition [209].

There are numerous studies on the shape memory behaviour of PLA, but few have explored the effects of FDM parameters on shape memory properties. Activation temperature, printed specimen thickness, and nozzle temperature have significantly impacted the shape recovery ratio and shape recovery rate of PLA. The shape recovery ratio is the ratio of the difference between original deformation and recovery deformation and shape recovery rate recovery in deformation per unit time [210].

Increasing activation temperature has been shown to improve shape recovery ratio in multiple cases. In a study based on the effects of operational parameters of FDM on 4D printing PLA, activation

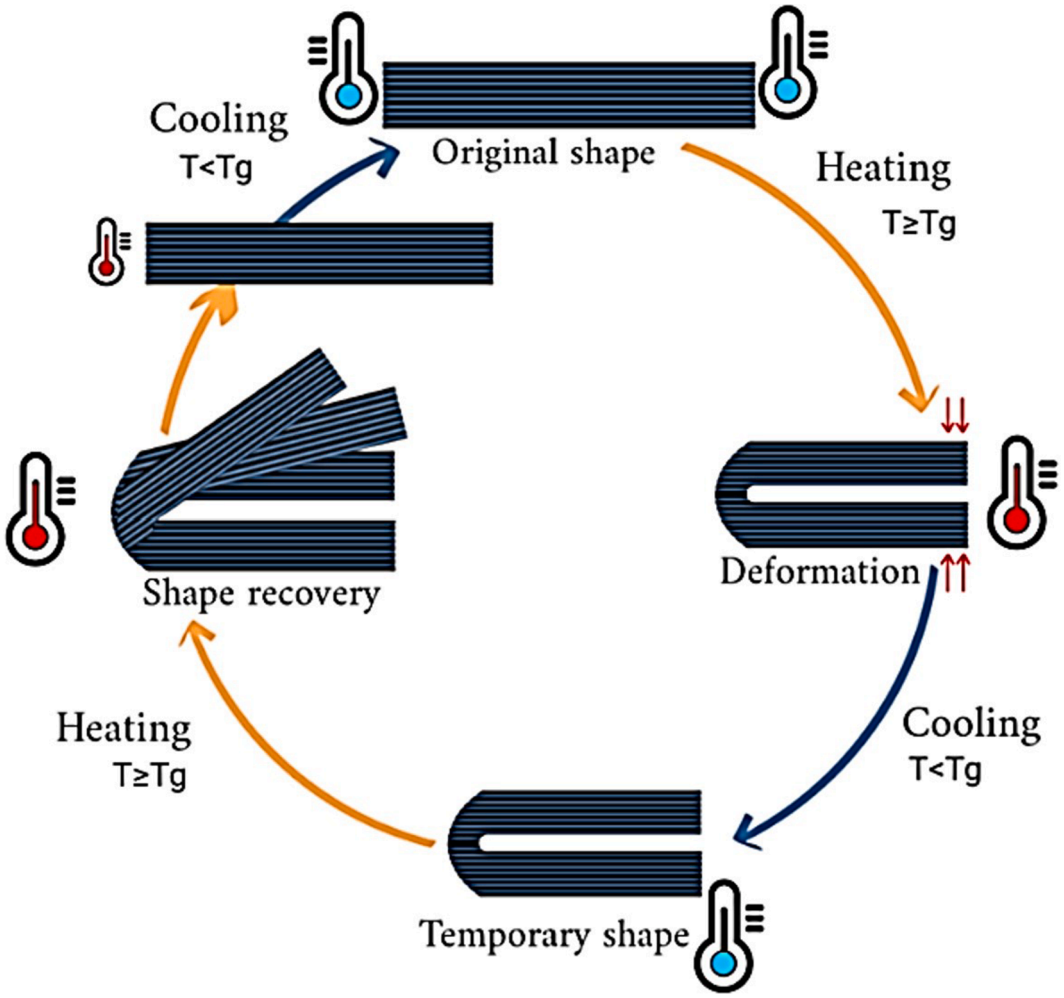


**Figure 21.** Shape-memory mechanism in PLA.

temperature was seen to have a significant effect on the shape recovery of PLA. A maximum of 99.3% recovery ratio was achieved at a temperature of 85°C [211]. Origami structure printed using PLA showed a recovery ratio of 85% at an activation temperature of 65°C, and when the temperature was increased to 75°C, full shape recovery was observed [212]. In another study investigating FDM 3D printed PLA honeycomb structure, an increase from 68% to 74% was recorded in shape recovery ratio when the activation temperature was increased from 65°C to 85°C [213].

3D printed part thickness was also seen to directly affect shape recovery. Shape recovery behaviour was analysed by printing PLA directly onto the print bed and printing PLA onto a nylon fabric. It was observed that the shape recovery percentage decreased with an increase in the thickness of the 3D printed sample. For both cases, 800μm thick samples showed the highest shape recovery ratio with 75.5% and 1200μm thick samples showed the lowest shape recovery ratio with 42.9% [49]. Another study on the effects of printing parameters on PLA shape recovery showed that layer thickness had a minimum influence on shape recovery ratio and more influence on the maximum shape recovery rate. The optimum layer thickness to get the best shape recovery ratio was observed to be 150 μm, and the optimum layer thickness to get the best maximum shape recovery rate was 300 μm [70].

Higher nozzle temperatures showed an improvement in the shape-recovery rate of PLA [211,213]. A 10% increase in shape recovery ratio was observed when nozzle temperature was increased from 175°C to 225°C. In another research, increasing nozzle temperature from 190°C to 210°C resulted in an increase in shape recovery ratio from 62% to 68%, but no further improvement was observed above 230°C [213]. Table 11 gives a summary of the main findings in recent research based on 4D printing PLA and its biocomposites using FDM.

PLA based hygromorphic composites (HBCs) can be 4D printed by using bio-derived reinforcements that display anisotropic swelling upon water absorption [217,218]. HBCs are based on the bilayer structure of natural fibres [219]. Recent work in HBCs includes wood fibre, spores, and natural fibres such as jute, flax, kenaf, and coir [53]. For HBCs, the responsiveness or the variation of curvature between the initial and final stages of initiation is determined by Timoshenko's equations as

$$\Delta\kappa = \Delta\beta \cdot \Delta C \cdot \frac{f(m,n)}{t} \tag{1}$$

$$f(m,n) = \frac{6(1+m)^2}{3(1+m)^2 + (1+mn) + \left(m^2 + \frac{1}{mn}\right)} \tag{2}$$

Here $\Delta\kappa$ is the change of curvature of the bilayer, $f$ (m, n) is a function that depends on various variables, including $m = \frac{t_p}{t_a}$ Where $t_p$ and $t_a$ are thicknesses of passive and active layers, respectively and $n = \frac{E_p}{E_a}$ where $E_p$ and $E_a$ are longitudinal Young's moduli of the wet passive and active layers. $\Delta\beta$ is the coefficient of differential hygroscopic expansion between the two layers, $\Delta C$ is the difference in moisture content in the storage and the testing environments, and $t$ is the thickness of the sample [53].

HBCs are 4D printed using two approaches – a mono-material approach and the multi-material approach. The mono-material approach is based on stacking the layers of the material in the printing process in an asymmetric manner to achieve anisotropy in the same printed material. Mono materials further have two categories – full material filling and partial filling. Actuation in the full material filling approach is dependent on printing orientation, the overlap of the filaments that control porosity, layer height, number of printed layers, and the raster angle [220]. For example, changing the overlap from positive to negative in a wood/PLA/PHA biocomposite increased the porosity content by 6±0.5%, reducing responsiveness due to the lowered swelling strains. Figure 22 shows a plot of maximum curvature ($K_{max}$) as a function of actuation speed for compressed samples and samples of different widths. It can be seen that higher porosity leads to faster actuation. Apart from the actuation speed, $K_{max}$ is also influenced by the width of the sample, hygroelastic properties, and the microstructure [217].

The partial filling approach in printing HBCs utilises filament anisotropy, the spacing between the filaments, interfilament bonding, and surface/volume ratio. For example, it was shown that increasing the printing path space from 1mm to 1.5mm improved the responsiveness of wood/PLA HBC [220].

The multi-material printing approach uses a hygroscopic material along with PLA that has low moisture absorption or swelling properties. To obtain maximum responsiveness, materials should be selected such that a high difference of hygroscopic strains between layers is obtained. However, the two materials must be compatible to prevent delamination. Hygroscopic material is oriented in the direction perpendicular to

**Table 11**
Summary of main findings in recent research in 4D printing PLA and its composites with bio-derived additives.

| Material | Type of responsiveness | Results | Key observations | Year | Ref. |
|---|---|---|---|---|---|
| PLA | Thermo-responsive | An add-on device was used to print on a curved surface, and the potential for 4D printing different types of reconfigurable devices was demonstrated. | Lower printing temperatures led to an increase in shrinkage. Shape memory behaviour was seen to largely depend on the activation medium used, and shape-shifting was achieved in short activation times, typically less than 30 seconds. | 2021 | [214] |
| PLA printed as a spring structure and a vase structure | Thermo-responsive | - | It was demonstrated that commercial PLA could be used as a shape memory polymer to 3D print complicated shapes | 2021 | [215] |
| PLLA | Thermo-responsive | Activation temperature has the highest effect on shape recovery time. | Along with activation temperature, nozzle temperature also plays a role in achieving a better shape recovery rate. Higher nozzle temperatures (210°C) favour shape recovery time and percentage | 2021 | [211] |
| PLA printed as a honey comb structure | Thermo-responsive | Up to 74% recovery ratio was obtained | Higher nozzle temperatures (210°C and above) resulted in higher unfolding rates, and higher activation temperatures (85°C) resulted in higher recovery rates. | 2020 | [213] |
| PLA origami structure | Thermo-responsive | A maximum of 90% shape recovery rate was achieved | Activation temperature plays a significant role in shape recovery. Nozzle temperature has less significance compared to factors like thickness and layer height. | 2020 | [212] |
| PLA/HA (Hydroxyapatite) | Thermo-responsive | 95.8% recovery achieved | Samples with 8wt% HA displayed maximum shape memory. Infill density was observed to have the highest influence on mechanical properties. | 2020 | [216] |

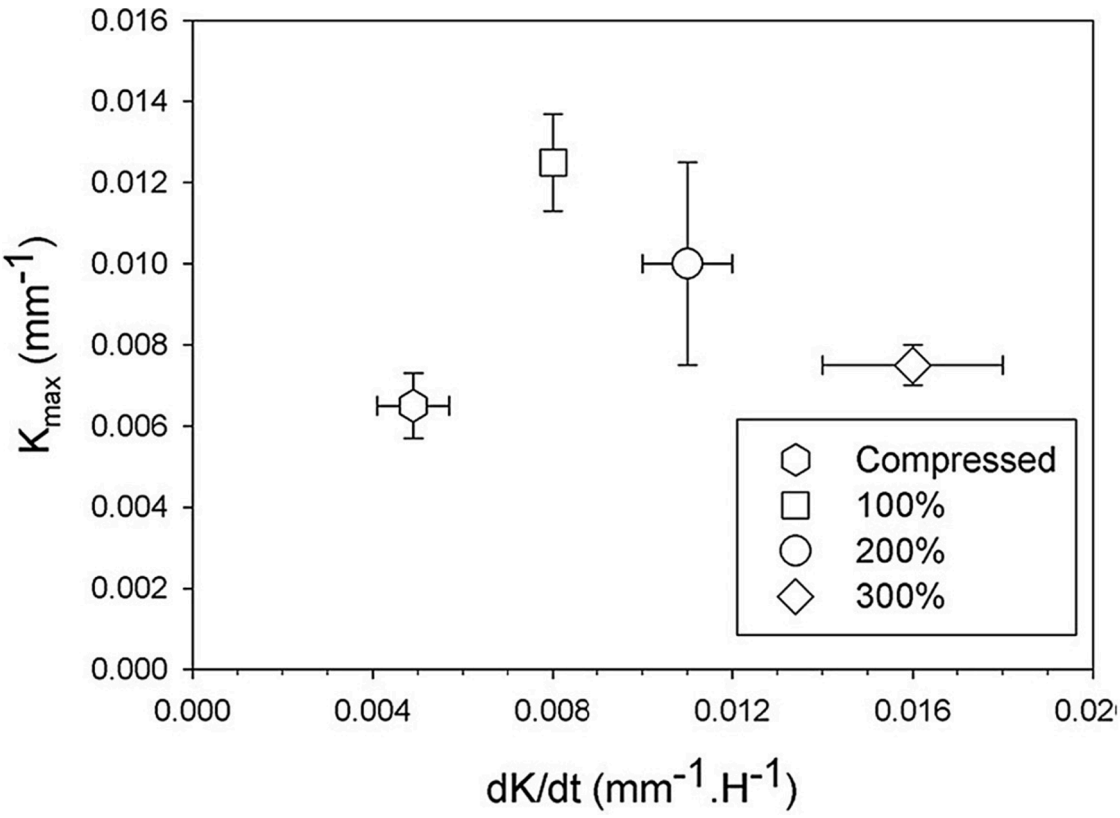


**Figure 22.** Maximum curvature (Kmax) as a function of actuation speed for compressed samples and samples of different widths [217]. Reproduced with permission from Elsevier, license number 5124230593451.

the desired direction of expansion, and the polymer is oriented in a direction parallel to the direction of expansion [218]. Bio-inspired multifunctional materials can be designed, and 3D printed using the multi-material approach. For example, wood-filled thermoplastic composites were designed and developed to obtain self-shaping orthotic splints. The hygroscopic nature of wood was exploited to demonstrate the principle of self-tightening observed in the Dioscorea bulbifera plant [221]. In another research work, a curling behaviour was observed on exposure to moisture in a flat composite sheet comprising PLA and wood fibre. Upon exposure to moisture, the polymer will constrain the expansion of the wood. This results in the improvement of control over the extent and direction of deformation [218]. Similar research was conducted using commercially available PLA/PHA (poly(hydroxyalkanoate))/wood composite filament for FDM 3D printing. It was observed that layer thickness and printing orientation significantly impact the mechanical properties of FDM 3D printed PLA/PHA/wood composite. High levels of porosity and moisture absorption were observed with a reduction in tensile strength [222].

Bio-derived fibre content is a significant factor to improve responsiveness in 4D printed HBCs. Since the bio-derived fibre acts as the actuator in HBCs, a high volume fraction is desirable to achieve faster and higher swelling [223]. However, the use of high volume fractions of discontinuous fibres leads to clogging, as discussed earlier. Using continuous bio-derived reinforcements can be an excellent strategy to achieve high responsiveness and avoid printer nozzle blocking [88]. Apart from the materials, the architecture of HBCs also plays an essential role in enhancing the responsiveness of HBCs [224]. Bio-inspired designs include movement of pine-cone scales by multi-stage double curvature, force generation principle in Dioscorea bulbifera plant, edge-growth propelled flower opening in the lily plant, curvature inversions from concave to convex to trap prey in venus flytrap, and others have been explored to produce HBCs [221,225]. However, the main challenges in combining 3D printing technologies and biomimetic designs include achieving enhanced actuation, functional robustness, and high mechanical properties [225].

## 6. Summary and Outlook

Additive manufacturing of biocomposites using FDM is currently a subject of growing research interest. Bio-derived materials have become popular due to their mechanical qualities, environmental benefits, and commercial viability. The use of PLA biocomposites has become increasingly common among various industrial sectors with growing interest in employing environmentally beneficial materials. Studies based on the use of bio-derived reinforcements for PLA matrix aim to achieve similar performance as their petroleum-based counterparts. This article presented a detailed overview of a range of bioderived reinforcements and their effects on the performance of FDM 3D printed PLA. The processing methodology and results for bio-derived fibre, particulate, and nanomaterial reinforcements have been outlined in detail. A comparison has been made between traditionally manufactured and 3D printed PLA biocomposite. In addition, an overview is presented on existing research, recent progress, and opportunities for future development of FDM 3D/4D printing of PLA and its biocomposites.

One of the main challenges for biocomposites using FDM is achieving tensile properties comparable to conventional processes such as compression moulding or injection moulding. Three major factors in achieving higher mechanical properties for FDM 3D printed PLA biocomposites are improving interfacial adhesion, using high strength bioderived reinforcements, and developing innovative ways of producing continuous fibre reinforced filaments. Discontinuous fibre reinforcements offer limited benefits in enhancing mechanical properties due to high porosity and anisotropy. Future research trends show the use of continuous fibre reinforcements to effectively improve the mechanical properties of FDM 3D printed PLA biocomposites. Current studies on

continuous bio-derived reinforcements employ commercially available fibre yarns, preferably with a low twist. Customised development of fibre yarns for 3D printing can be an alternative to commercial yarns. Investigation in the area of production of continuous natural fibre reinforced PLA filaments is in the initial stages, and further research is required to achieve high fibre content filaments.

4D Printing offers the advantages of combining complex design manufacturing and the potential to produce self-actuating objects. The future of 4D printing biocomposites involves multi-disciplinary research to combine design strategies, material properties, stimulus properties, and composite mechanics. PLA biocomposites are very promising for FDM 4D printing since PLA displays a shape memory effect and the use of bio-derived reinforcements allows exploration of the hygromorphic nature of the printed composites. Biocomposites that respond to applied external stimulus in a useful manner can be produced by exploiting the tendency of natural fibres to behave as hydraulic actuators. Complex material architectures can be researched by controlling fibre orientation and distribution. Potential research opportunities include control of actuation, improvement of actuation performance by increased fibre content and better material selection.

## Declaration of competing interests

The authors declare that they have no known competing financial interests or personal relationships that could have appeared to influence the work reported in this paper.

## Acknowledgements

The authors would like to thank the financial support from the Ministry of Business, Innovation and Employment of New Zealand through the National Science Challenge spearhead project “Additive manufacturing and 3D and/or 4D printing of bio-composites’ [grant 2019-S5-CRS] and The University of Waikato for the development of this paper.

## Supplementary materials

Supplementary material associated with this article can be found, in the online version, at doi:10.1016/j.jcomc.2022.100271.

## References

[1] G.C. Dumitrescu, I.A. Tanase, 3D Printing – A New Industrial Revolution, Knowl. Horizons. Econ. 8 (2016) 32–39. https://econpapers.repec.org/article/khejournl/v_3a8_3ay_3a2016_3ai_3a1_3ap_3a32-39.htm.

[2] T. Pereira, J.V. Kennedy, J. Potgieter, A comparison of traditional manufacturing vs additive manufacturing, the best method for the job, Procedia Manuf 30 (2019) 11–18, https://doi.org/10.1016/j.promfg.2019.02.003.

[3] N. Shahrubudin, T.C. Lee, R. Ramlan, An overview on 3D printing technology: Technological, materials, and applications, Procedia Manuf. 35 (2019) 1286–1296. https://doi.org/10.1016/j.promfg.2019.06.089.

[4] Z.X. Low, Y.T. Chua, B.M. Ray, D. Mattia, I.S. Metcalfe, D.A. Patterson, Perspective on 3D printing of separation membranes and comparison to related unconventional fabrication techniques, J. Memb. Sci. 523 (2017) 596–613, https://doi.org/10.1016/j.memsci.2016.10.006.

[5] S.A.M. Tofail, E.P. Koumoulos, A. Bandyopadhyay, S. Bose, L. O’Donoghue, C. Charitidis, Additive manufacturing: scientific and technological challenges, market uptake and opportunities, Mater. Today. 21 (2018) 22–37, https://doi.org/10.1016/j.mattod.2017.07.001.

[6] S.L. Sing, C.F. Tey, J.H.K. Tan, S. Huang, W.Y. Yeong, 2 - 3D printing of metals in rapid prototyping of biomaterials: Techniques in additive manufacturing, in: R. Narayan (Ed.), Rapid Prototyp. Biomater, Second Ed, Woodhead Publishing, 2020, pp. 17–40, https://doi.org/10.1016/B978-0-08-102663-2.00002-2, https://doi.org/https://doi.org/.

[7] W.T. Nugroho, Y. Dong, A. Pramanik, Chapter 4 - 3D printing composite materials: A comprehensive review, in: I.-M. Low, Y. Dong (Eds.), Compos. Mater, Elsevier, 2021, pp. 65–115, https://doi.org/10.1016/B978-0-12-820512-9.00013-7, https://doi.org/https://doi.org/.

[8] W. Jo, K.S. Chu, H.J. Lee, 3D and 4D Printing Technologies: An Overview, Material Matters 11 (2) (2016). https://www.sigmaaldrich.com/technical-documents/articles/material-matters/3d-and-4d-printing-technologies.html.

[9] Y. Zhang, W. Jarosinski, Y.-G. Jung, J. Zhang, 2 - Additive manufacturing processes and equipment, in: J. Zhang, Y.-G. Jung (Eds.), Additive Manufacturing., Butterworth-Heinemann, 2018, pp. 39–51, https://doi.org/10.1016/B978-0-12-812155-9.00002-5, https://doi.org/https://doi.org/.

[10] M. Sireesha, J. Lee, A.S. Kranthi Kiran, V.J. Babu, B.B.T. Kee, S. Ramakrishna, A review on additive manufacturing and its way into the oil and gas industry, RSC Adv 8 (2018) 22460–22468, https://doi.org/10.1039/c8ra03194k.

[11] R.M. Mahamood, T.C. Jen, S.A. Akinlabi, S. Hassan, K.O. Abdulrahman, E. T. Akinlabi, Chapter 6 - Role of additive manufacturing in the era of Industry 4.0, in: M. Manjaiah, K. Raghavendra, N. Balashanmugam, J.P. Davim (Eds.), Additive Manufacturing, Woodhead Publishing, 2021, pp. 107–126, https://doi.org/10.1016/B978-0-12-822056-6.00003-5, https://doi.org/https://doi.org/.

[12] A. Al Rashid, W. Ahmed, M.Y. Khalid, M. Koç, Vat photopolymerization of polymers and polymer composites: Processes and applications, Addit. Manuf. 47 (2021), 102279, https://doi.org/10.1016/j.addma.2021.102279 https://doi.org/https://doi.org/.

[13] N. Oxman, J. Laucks, M. Kayser, E. Tsai, M. Firstenberg, Freeform 3D printing: Towards a sustainable approach to additive manufacturing, Green Des. Mater. Manuf. Process. - Proc. 2nd Int. Conf. Sustain, Intell. Manuf (2013) 479–483. SIM 2013.

[14] Kuka Partner Publishes Video on Using Freeform 3D Printing for the Future of Construction, 3D Print. Media Netw. (2016). https://www.3dprintingmedia.network/kuka-releases-video-using-robotic-arm-additive-building-construction. (accessed August 26, 2020).

[15] W. Jo, K.S. Chu, H.J. Lee, 3D and 4D Printing Technologies: An Overview, Material Matters 11 (2) (2016) https://www.sigmaaldrich.com/technical-documents/articles/material-matters/3d-and-4d-printing-technologies.html#:~:text=3D printing can involve different,the design process more important.

[16] S.C. Ligon, R. Liska, J. Stampfl, M. Gurr, R. Mülhaupt, Polymers for 3D Printing and Customized Additive Manufacturing, Chem. Rev. 117 (2017) 10212–10290, https://doi.org/10.1021/acs.chemrev.7b00074.

[17] T.A. Campbell, S. Tibbits, B. Garrett, The next wave : 4D printing - programming the material world, Atl. Counc. (2014) 1–15. https://www.atlanticcouncil.org/wp-content/uploads/2014/05/The_Next_Wave_4D_Printing_Programming_the_Material_World.pdf.

[18] R. Bogue, Smart materials: A review of capabilities and applications, Assem. Autom. 34 (2014) 16–22, https://doi.org/10.1108/AA-10-2013-094.

[19] N.Z. Nkomo, A review of 4D printing technology and future trends, National University of Science and Technology, Zimbabwe, 2018. https://www.researchgate.net/publication/328162917%0AA.

[20] X. Li, J. Shang, Z. Wang, Intelligent materials: A review of applications in 4D printing, Assem. Autom. 37 (2017) 170–185, https://doi.org/10.1108/AA-11-2015-093.

[21] S. Tibbits, C. McKnelly, C. Olguin, D. Dikovsky, S. Hirsch, 4D printing and universal transformation, ACADIA 2014 - Des. Agency Proc. 34th Annu. Conf. Assoc. Comput. Aided Des. Archit, 2014-Octob (2014) 539–548.

[22] F. Momeni, S. M.Mehdi Hassani.N, X. Liu, J. Ni, A review of 4D printing, Mater. Des. 122 (2017) 42–79, https://doi.org/10.1016/j.matdes.2017.02.068.

[23] J.E.M. Teoh, J. An, X. Feng, Y. Zhao, C.K. Chua, Y. Liu, Design and 4D printing of cross-folded origami structures: A preliminary investigation, Materials (Basel) 11 (2018), https://doi.org/10.3390/ma11030376.

[24] W.J. Grigsby, S.M. Scott, M.I. Plowman-Holmes, P.G. Middlewood, K. Recabar, Combination and processing keratin with lignin as biocomposite materials for additive manufacturing technology, Acta Biomater 104 (2020) 95–103, https://doi.org/10.1016/j.actbio.2019.12.026.

[25] Z. Zhang, K.G. Demir, G.X. Gu, Developments in 4D-printing: a review on current smart materials, technologies, and applications, Int. J. Smart Nano Mater. 10 (2019) 205–224, https://doi.org/10.1080/19475411.2019.1591541.

[26] A.V. Wijk, I.V. Wijk, 3D printing with biomaterials: Towards a sustainable and circular economy, IOS Press, 2015, https://doi.org/10.3233/978-1-61499-486-2-i.

[27] L. Columbus, The State of 3D Printing, 2018, Forbes (2018). https://www.forbes.com/sites/louiscolumbus/2018/05/30/the-state-of-3d-printing-2018/?sh=70f203a97b0a (accessed November 10, 2020).

[28] D. Chhabra, Comparison and analysis of different 3d printing techniques, Int. J. Latest Trends Eng. Technol. 8 (2017) 264–272, https://doi.org/10.21172/1.841.44.

[29] E. Gkartzou, E.P. Koumoulos, C.A. Charitidis, Production and 3D printing processing of bio-based thermoplastic filament, Manuf. Rev. (2017) 4, https://doi.org/10.1051/mfreview/2016020.

[30] Worldwide most used 3D printing materials, as of July 2018*, Statista. (2018). https://www.statista.com/statistics/800454/worldwide-most-used-3d-printing-materials/#:~:text=This statistic shows the worldwide,most used 3D printing material. (accessed September 2, 2020).

[31] E. Bugnicourt, P. Cinelli, A. Lazzeri, V. Alvarez, Polyhydroxyalkanoate (PHA): Review of synthesis, characteristics, processing and potential applications in packaging, Express Polym. Lett. 8 (2014) 791–808, https://doi.org/10.3144/expresspolymlett.2014.82.

[32] L.V. S. Pratt, B. Laycock, L. P. Halley, P. Lant, PHA Bioplastics - Synthesis and Material Properties, Presentation, University of Queensland (Australia) and AnoxKaldness (Sweden) https://d2cax41o7ahm5l.cloudfront.net/cs/speaker-ppts/steven-pratt-the-university-of-queensland-australia.pptx.

[33] D. Filgueira, S. Holmen, J.K. Melbø, D. Moldes, A.T. Echtermeyer, G. Chinga-Carrasco, 3D printable filaments made of biobased polyethylene biocomposites, Polymers (Basel) 10 (2018), https://doi.org/10.3390/polym10030314.

[34] F. Kucherov, E. Gordeev, A. Kashin, V. Ananikov, 3D printing with biobased PEF for carbon neutral manufacturing, Angew. Chemie Int. Ed 56 (2017), https://doi.org/10.1002/anie.201708528.

[35] S.J. Park, J.E. Lee, H.B. Lee, J. Park, N.K. Lee, Y. Son, S.H. Park, 3D printing of bio-based polycarbonate and its potential applications in ecofriendly indoor manufacturing, Addit. Manuf. 31 (2020), 100974, https://doi.org/10.1016/j.addma.2019.100974.

[36] sculpteo, Ultrasint® PA11 3D printing material, (2017). https://www.sculpteo.com/en/materials/sls-material/pa11/(accessed January 25, 2020).

[37] S.P. Dubey, V.K. Thakur, S. Krishnaswamy, H.A. Abhyankar, V. Marchante, J. L. Brighton, Progress in environmental-friendly polymer nanocomposite material from PLA: Synthesis, processing and applications, Vacuum 146 (2017) 655–663, https://doi.org/10.1016/j.vacuum.2017.07.009.

[38] S. Farah, D.G. Anderson, R. Langer, Physical and mechanical properties of PLA, and their functions in widespread applications — A comprehensive review, Adv. Drug Deliv. Rev. 107 (2016) 367–392, https://doi.org/10.1016/j.addr.2016.06.012, https://doi.org/https://doi.org/.

[39] E.B. Bezerra, D.C. de França, D.D. de Souza Morais, I.D. dos Santo Silva, D. D. Siqueira, E.M. Araújo, R.M.R. Wellen, Compatibility and characterization of Bio-PE/PCL blends, Polimeros (2019) 29, https://doi.org/10.1590/0104-1428.02518.

[40] R.B S.K. Patrycja Bazan *, Dariusz Mierzwiński, Bio-Based Polyethylene Composites with Natural Fiber: Mechanical, Thermal, and Ageing Properties, Materials (Basel) 13 (2020), https://doi.org/10.3390/ma13112595. https://doi.org/https://doi.org/.

[41] G. Wang, M. Jiang, Q. Zhang, R. Wang, G. Zhou, Biobased copolyesters: synthesis, crystallization behavior, thermal and mechanical properties of poly(ethylene glycol sebacate-co-ethylene glycol 2,5-furan dicarboxylate), RSC Adv 7 (2017) 13798–13807, https://doi.org/10.1039/c6ra27795k.

[42] O. Hauenstein, S. Agarwal, A. Greiner, Bio-based polycarbonate as synthetic toolbox, Nat. Commun. 7 (2016) 1–7, https://doi.org/10.1038/ncomms11862.

[43] Y.H. Choi, M.Y. Lyu, Comparison of Rheological Characteristics and Mechanical Properties of Fossil-Based and Bio-Based Polycarbonate, Macromol. Res. 28 (2020) 299–309, https://doi.org/10.1007/s13233-020-8093-1.

[44] S. Wickramasinghe, T. Do, P. Tran, FDM-Based 3D printing of polymer and associated composite: A review on mechanical properties, defects and treatments, Polymers (Basel) 12 (2020) 1–42, https://doi.org/10.3390/polym12071529.

[45] T. Mukherjee, N. Kao, PLA Based Biopolymer Reinforced with Natural Fibre: A Review, J. Polym. Environ. 19 (2011) 714–725, https://doi.org/10.1007/s10924-011-0320-6.

[46] A.S. Getme, B. Patel, A review: Bio-fiber's as reinforcement in composites of polylactic acid (PLA), Mater. Today Proc 26 (2019) 2116–2122, https://doi.org/10.1016/j.matpr.2020.02.457.

[47] X. Wu, W.M. Huang, Y. Zhao, Z. Ding, C. Tang, J. Zhang, Mechanisms of the shape memory effect in polymeric materials, Polymers (Basel) 5 (2013) 1169–1202, https://doi.org/10.3390/polym5041169.

[48] J. Zhou, S. Sheiko, Reversible shape-shifting in polymeric materials, J. Polym. Sci. Part B Polym. Phys. 54 (2016), https://doi.org/10.1002/polb.24014 n/a-n/a.

[49] S.K. Leist, D. Gao, R. Chiou, J. Zhou, Investigating the shape memory properties of 4D printed polylactic acid (PLA) and the concept of 4D printing onto nylon fabrics for the creation of smart textiles, Virtual Phys. Prototyp. 12 (2017) 290–300, https://doi.org/10.1080/17452759.2017.1341815.

[50] C. Yang, B. Wang, D. Li, X. Tian, Modelling and characterisation for the responsive performance of CF/PLA and CF/PEEK smart materials fabricated by 4D printing, Virtual Phys. Prototyp. 12 (2017) 69–76, https://doi.org/10.1080/17452759.2016.1265992.

[51] S.K. Dogan, S. Boyacioglu, M. Kodal, O. Gokce, G. Ozkoc, Thermally induced shape memory behavior, enzymatic degradation and biocompatibility of PLA/TPU blends: "Effects of compatibilization, J. Mech. Behav. Biomed. Mater. 71 (2017) 349–361, https://doi.org/10.1016/j.jmbbm.2017.04.001.

[52] F.S. Senatov, K.V. Niaza, M.Y. Zadorozhnyy, A.V. Maksimkin, S.D. Kaloshkin, Y. Z. Estrin, Mechanical properties and shape memory effect of 3D-printed PLA-based porous scaffolds, J. Mech. Behav. Biomed. Mater. 57 (2016) 139–148, https://doi.org/10.1016/j.jmbbm.2015.11.036.

[53] A.Le Duigou, M. Castro, Moisture-induced self-shaping flax-reinforced polypropylene biocomposite actuator, Ind. Crops Prod. 71 (2015) 1–6, https://doi.org/10.1016/j.indcrop.2015.03.077.

[54] J.W.C. Dunlop, R. Weinkamer, P. Fratzl, Artful interfaces within biological materials, Mater. Today. 14 (2011) 70–78, https://doi.org/10.1016/S1369-7021(11)70056-6.

[55] T.N.A.T. Rahim, A.M. Abdullah, H.Md Akil, Recent Developments in Fused Deposition Modeling-Based 3D Printing of Polymers and Their Composites, Polym. Rev. 59 (2019) 589–624, https://doi.org/10.1080/15583724.2019.1597883.

[56] B. Road, a Review : Fused Deposition Modeling – a Rapid Prototyping Process, Int. Res. J. Eng. Technol. 4 (2017) 5–9. https://irjet.net/archives/V4/i9/IRJET-V4I989.pdf.

[57] T.N. Tran, J. Heredia-Guerrero, M. Frugone, M. Lagomarsino, F. Maggio, A. Athanassiou, Cocoa Shell Waste Biofilaments for 3D Printing Applications, Macromol. Mater. Eng. 302 (2017), 1700219, https://doi.org/10.1002/mame.201700219.

[58] J. Hart, 3D Printing History at MIT, Additive Manufacturing, October 21, 2019, Presentation. http://web.mit.edu/2.810/www/files/lectures/lec10b-fdm-2019.pdf (accessed August 12, 2020).

[59] F. Ning, W. Cong, J. Wei, S. Wang, M. Zhang, Additive Manufacturing of CFRP Composites Using Fused Deposition Modeling: Effects of Carbon Fiber Content and Length, (2015). https://doi.org/10.1115/msec2015-9436.

[60] Z. Liu, Y. Wang, B. Wu, C. Cui, Y. Guo, C. Yan, A critical review of fused deposition modeling 3D printing technology in manufacturing polylactic acid parts, Int. J. Adv. Manuf. Technol. 102 (2019) 2877–2889, https://doi.org/10.1007/s00170-019-03332-x.

[61] D. Popescu, A. Zapciu, C. Amza, F. Baciu, R. Marinescu, FDM process parameters influence over the mechanical properties of polymer specimens: A review, Polym. Test. 69 (2018) 157–166, https://doi.org/10.1016/j.polymertesting.2018.05.020.

[62] B. Akhoundi, A.H. Behravesh, Effect of Filling Pattern on the Tensile and Flexural Mechanical Properties of FDM 3D Printed Products, Exp. Mech. 59 (2019) 883–897, https://doi.org/10.1007/s11340-018-00467-y.

[63] M. Samykano, S.K. Selvamani, K. Kadirgama, W.K. Ngui, G. Kanagaraj, K. Sudhakar, Mechanical property of FDM printed ABS: influence of printing parameters, Int. J. Adv. Manuf. Technol. 102 (2019) 2779–2796, https://doi.org/10.1007/s00170-019-03313-0.

[64] V. Mazzanti, L. Malagutti, F. Mollica, FDM 3D printing of polymers containing natural fillers: A review of their mechanical properties, Polymers (Basel) 11 (2019), https://doi.org/10.3390/polym11071094.

[65] C. Luo, Modeling the temperature profile of an extrudate in material extrusion additive manufacturing, Mater. Lett. 270 (2020), 127742, https://doi.org/10.1016/j.matlet.2020.127742.

[66] I.J. Solomon, P. Sevvel, J. Gunasekaran, A review on the various processing parameters in FDM, Mater, Today Proc 37 (2020) 509–514, https://doi.org/10.1016/j.matpr.2020.05.484.

[67] M. Domingo-Espin, J.M. Puigoriol-Forcada, A.-A. Garcia-Granada, J. Llumà, S. Borros, G. Reyes, Mechanical property characterization and simulation of fused deposition modeling Polycarbonate parts, Mater. Des. 83 (2015) 670–677, https://doi.org/10.1016/j.matdes.2015.06.074, https://doi.org/https://doi.org/.

[68] W.C. Smith, R.W. Dean, Structural characteristics of fused deposition modeling polycarbonate material, Polym. Test. 32 (2013) 1306–1312, https://doi.org/10.1016/j.polymertesting.2013.07.014, https://doi.org/https://doi.org/.

[69] Y. Jin, Y. Wan, B. Zhang, Z. Liu, Modeling of the chemical finishing process for polylactic acid parts in fused deposition modeling and investigation of its tensile properties, J. Mater. Process. Technol. 240 (2017) 233–239, https://doi.org/10.1016/j.jmatprotec.2016.10.003, https://doi.org/https://doi.org/.

[70] W. Wu, W. Ye, Z. Wu, P. Geng, Y. Wang, J. Zhao, Influence of layer thickness, raster angle, deformation temperature and recovery temperature on the shape-memory effect of 3D-printed polylactic acid samples, Materials (Basel) 10 (2017), https://doi.org/10.3390/ma10080970.

[71] W. Wu, P. Geng, G. Li, D. Zhao, H. Zhang, J. Zhao, Influence of layer thickness and raster angle on the mechanical properties of 3D-printed PEEK and a comparative mechanical study between PEEK and ABS, Materials (Basel) 8 (2015) 5834–5846, https://doi.org/10.3390/ma8095271.

[72] J.R.C. Dizon, A.H. Espera, Q. Chen, R.C. Advincula, Mechanical characterization of 3D-printed polymers, Addit. Manuf. 20 (2018) 44–67, https://doi.org/10.1016/j.addma.2017.12.002, https://doi.org/https://doi.org/.

[73] N.K. Maurya, V. Rastogi, P. Singh, An overview of mechanical properties and form error for rapid prototyping, CIRP J. Manuf. Sci. Technol. 29 (2020) 53–70, https://doi.org/10.1016/j.cirpj.2020.02.003, https://doi.org/https://doi.org/.

[74] C. Dudescu, L. Racz, Effects of Raster Orientation, Infill Rate and Infill Pattern on the Mechanical Properties of 3D Printed Materials, ACTA Univ. Cibiniensis. 69 (2018) 23–30, https://doi.org/10.1515/aucts-2017-0004.

[75] M. Ouhsti, B. El Haddadi, S. Belhouideg, Effect of printing parameters on the mechanical properties of parts fabricated with open-source 3D printers in PLA by fused deposition modeling, Mech. Mech. Eng. 22 (2018) 895–907, https://doi.org/10.2478/mme-2018-0070.

[76] N. Mohan, P. Senthil, S. Vinodh, N. Jayanth, A review on composite materials and process parameters optimisation for the fused deposition modelling process, Virtual Phys. Prototyp. 12 (2017) 47–59, https://doi.org/10.1080/17452759.2016.1274490.

[77] T.-C. Yang, C.-H. Yeh, Morphology and Mechanical Properties of 3D Printed Wood Fiber/Polylactic Acid Composite Parts Using Fused Deposition Modeling (FDM): The Effects of Printing, Polymers (Basel) (2020), https://doi.org/10.3390/polym12061334.

[78] P. Geng, J. Zhao, W. Wu, W. Ye, Y. Wang, S. Wang, S. Zhang, Effects of extrusion speed and printing speed on the 3D printing stability of extruded PEEK filament, J. Manuf. Process. 37 (2019) 266–273, https://doi.org/10.1016/j.jmapro.2018.11.023, https://doi.org/https://doi.org/.

[79] Ł. Miazio, Impact of Print Speed on Strength of Samples Printed in FDM Technology, Agric. Eng. 23 (2019) 33–38, https://doi.org/10.1515/agriceng-2019-0014.

[80] A. Pappu, K.L. Pickering, V.K. Thakur, Manufacturing and characterization of sustainable hybrid composites using sisal and hemp fibres as reinforcement of poly (lactic acid) via injection moulding, Ind. Crops Prod. 137 (2019) 260–269, https://doi.org/10.1016/j.indcrop.2019.05.040.

[81] D. Garlotta, A Literature Review of Poly(Lactic Acid), J. Polym. Environ 9 (2022), https://doi.org/10.1023/A:1020200822435 n.d.

[82] K.M Y. Kimura*a, PLA Synthesis, From the Monomer to the Polymer, Oly(Lactic Acid) Sci. Technol. Process. Prop. Addit. Appl. (2014) 1–36, https://doi.org/10.1039/9781782624806-00001.

[83] M. Murariu, P. Dubois, PLA composites, From production to properties, Adv. Drug Deliv. Rev. 107 (2016) 17–46, https://doi.org/10.1016/j.addr.2016.04.003.

[84] M.H. Hartmann, High Molecular Weight Polylactic Acid Polymers, in: D.L. Kaplan (Ed.), Biopolym. from Renew. Resour, Springer, Berlin Heidelberg, Berlin, Heidelberg, 1998, pp. 367–411, https://doi.org/10.1007/978-3-662-03680-8_15.
[85] K. Madhavan Nampoothiri, N.R. Nair, R.P. John, An overview of the recent developments in polylactide (PLA) research, Bioresour. Technol. 101 (2010) 8493–8501, https://doi.org/10.1016/j.biortech.2010.05.092.
[86] P.D Pastuszak, Aleksander Muc, Application of Composite Materials in Modern Constructions, Key Engineering Materials 542 (2013) 119–129, https://doi.org/10.4028/www.scientific.net/KEM.542.119.
[87] L. Kerni, S. Singh, A. Patnaik, N. Kumar, A review on natural fiber reinforced composites, Mater. Today Proc 28 (2020) 1616–1621, https://doi.org/10.1016/j.matpr.2020.04.851.
[88] A.Le Duigou, D. Correa, M. Ueda, R. Matsuzaki, M. Castro, A review of 3D and 4D printing of natural fibre biocomposites, Mater. Des. 194 (2020), 108911, https://doi.org/10.1016/j.matdes.2020.108911.
[89] M.R. Vengatesan, V. Mittal, Nanoparticle- and Nanofiber-Based Polymer Nanocomposites: An Overview, in, Spherical Fibrous Fill. Compos (2016) 1–38, https://doi.org/10.1002/9783527670222.ch1, https://doi.org/https://doi.org/.
[90] S.K. Ramamoorthy, M. Skrifvars, A. Persson, A review of natural fibers used in biocomposites: Plant, animal and regenerated cellulose fibers, Polym. Rev. 55 (2015) 107–162, https://doi.org/10.1080/15583724.2014.971124.
[91] K.L. Pickering, M.G.A. Efendy, T.M. Le, A review of recent developments in natural fibre composites and their mechanical performance, Composites. Part A Appl. Sci. Manuf. 83 (2016) 98–112, https://doi.org/10.1016/j.compositesa.2015.08.038.
[92] C. Gauss, K.L. Pickering, L.P. Muthe, The use of cellulose in bio-derived formulations for 3D/4D printing: A review, Compos. Part C Open Access. 4 (2021), 100113, https://doi.org/10.1016/j.jcomc.2021.100113.
[93] A.J. Sayyed, N.A. Deshmukh, D.V. Pinjari, A critical review of manufacturing processes used in regenerated cellulosic fibres: viscose, cellulose acetate, cuprammonium, LiCl/DMAc, ionic liquids, and NMMO based lyocell, Cellulose 26 (2019) 2913–2940, https://doi.org/10.1007/s10570-019-02318-y.
[94] A. Lotfi, H. Li, D.V. Dao, G. Prusty, Natural fiber–reinforced composites: A review on material, manufacturing, and machinability, J. Thermoplast. Compos. Mater. 34 (2021) 238–284, https://doi.org/10.1177/0892705719844546.
[95] T. Khan, M.T. Bin Hameed Sultan, A.H. Ariffin, The challenges of natural fiber in manufacturing, material selection, and technology application: A review, J. Reinf. Plast. Compos. 37 (2018) 770–779, https://doi.org/10.1177/0731684418756762.
[96] R. Vijayan, A. Krishnamoorthy, Review on natural fiber reinforced composites, Mater. Today Proc. 16 (2019) 897–906, https://doi.org/10.1016/j.matpr.2019.05.175.
[97] G. Jiang, W. Huang, L. Li, X. Wang, F. Pang, Y. Zhang, H. Wang, Structure and properties of regenerated cellulose fibers from different technology processes, Carbohydr. Polym. 87 (2012) 2012–2018, https://doi.org/10.1016/j.carbpol.2011.10.022, https://doi.org/https://doi.org/.
[98] R.B. Adusumali, M. Reifferscheid, H. Weber, T. Roeder, H. Sixta, W. Gindl, Mechanical properties of regenerated cellulose fibres for composites, Macromol. Symp. 244 (2006) 119–125, https://doi.org/10.1002/masy.200651211.
[99] R.B. Adusumalli, U. Müller, H. Weber, T. Roeder, H. Sixta, W. Gindl, Tensile testing of single regenerated cellulose fibres, Macromol. Symp. 244 (2006) 83–88, https://doi.org/10.1002/masy.200651207.
[100] A. Gomes, T. Matsuo, K. Goda, J. Ohgi, Development and effect of alkali treatment on tensile properties of curaua fiber green composites, Compos. Part A Appl. Sci. Manuf. 38 (2007) 1811–1820, https://doi.org/10.1016/j.compositesa.2007.04.010.
[101] M. a S. Spinacé, C.S. Lambert, K.K.G. Fermoselli, M. a. De Paoli, Characterization of lignocellulosic curaua fibres, Carbohydr. Polym. 77 (2009) 47–53, https://doi.org/10.1016/j.carbpol.2008.12.005.
[102] E.O. Cisneros-López, A.K. Pal, A.U. Rodriguez, F. Wu, M. Misra, D.F. Mielewski, A. Kiziltas, A.K. Mohanty, Recycled poly(lactic acid)–based 3D printed sustainable biocomposites: a comparative study with injection molding, Mater. Today Sustain. 7–8 (2020) 1–12, https://doi.org/10.1016/j.mtsust.2019.100027.
[103] B. Coppola, E. Garofalo, L. Di Maio, P. Scarfato, L. Incarnato, Investigation on the use of PLA/hemp composites for the fused deposition modelling (FDM) 3D printing, in: AIP Conf. Proc. 1981, 2018, pp. 1–5, https://doi.org/10.1063/1.5045948.
[104] T.-C.Y. C.-H. Yeh, Morphology and Mechanical Properties of 3D Printed Wood Fiber/Polylactic Acid Composite Parts Using Fused Deposition Modeling (FDM): The Effects of Printing Speed Polymers (Basel) (2020) https://doi.org/10.3390/polym12061334.
[105] C. Wang, L.M. Smith, W. Zhang, M. Li, G. Wang, S.Q. Shi, H. Cheng, S. Zhang, Reinforcement of polylactic acid for fused deposition modeling process with nano particles treated bamboo powder, Polymers (Basel) 11 (2019), https://doi.org/10.3390/polym11071146.
[106] R.J. Moon, A. Martini, J. Nairn, J. Simonsen, J. Youngblood, Cellulose nanomaterials review: Structure, properties and nanocomposites, 2011. https://doi.org/10.1039/c0cs00108b.
[107] F.V. Ferreira, I.F. Pinheiro, R.F. Gouveia, G.P. Thim, L.M.F. Lona, Functionalized cellulose nanocrystals as reinforcement in biodegradable polymer nanocomposites, Polym. Compos. 39 (2018) E9–E29, https://doi.org/10.1002/pc.24583.
[108] P.M. Spasojevic, Chapter 15 - Thermal and Rheological Properties of Unsaturated Polyester Resins-Based Composites, in: S. Thomas, M. Hosur, C.J. Chirayil (Eds.), Unsaturated Polyest. Resins, Elsevier, 2019, pp. 367–406, https://doi.org/10.1016/B978-0-12-816129-6.00015-6, https://doi.org/https://doi.org/.
[109] M. Sharma, D. Verma, H. Sharma, A.K. Chaudhary, 6 - Roadmap for materials selection, processing, and utilization of biocompatible composites in biomedical sectors, in: D. Verma, M. Sharma, K.L. Goh, S. Jain, H. Sharma (Eds.), Sustain. Biopolym. Compos., Woodhead Publishing, 2022, pp. 129–152, https://doi.org/10.1016/B978-0-12-822291-1.00006-3, https://doi.org/https://doi.org/.
[110] S. Ebnesajjad, 7 - Injection Molding, in: S. Ebnesajjad (Ed.), Melt Process. Fluoroplastics, William Andrew Publishing, Norwich, NY, 2003, pp. 151–193, https://doi.org/10.1016/B978-188420796-9.50010-2, https://doi.org/https://doi.org/.
[111] D.Stoof Y.Zhang, K.L. Pickering, Fused Deposition Modelling of Natural Fibre/Polylactic Acid Composites, J. Compos. Sci. 1 (2017) 8, https://doi.org/10.3390/jcs1010008.
[112] Q. Wang, C. Ji, L. Sun, J. Sun, J. Liu, Cellulose nanofibrils filled poly(lactic acid) biocomposite filament for FDM 3D printing, Molecules 25 (2020), https://doi.org/10.3390/molecules25102319.
[116] D. Depuydt, M. Balthazar, K. Hendrickx, W. Six, E. Ferraris, F. Desplentere, J. Ivens, A.W. Van Vuure, Production and characterization of bamboo and flax fiber reinforced polylactic acid filaments for fused deposition modeling (FDM), Polym. Compos. 40 (2019) 1951–1963, https://doi.org/10.1002/pc.24971.
[117] K.L. Pickering, M.G. Aruan Efendy, Preparation and mechanical properties of novel bio-composite made of dynamically sheet formed discontinuous harakeke and hemp fibre mat reinforced PLA composites for structural applications, Ind. Crops Prod. 84 (2016) 139–150, https://doi.org/10.1016/j.indcrop.2016.02.005.
[118] E. Hassan, Plant Fibers Reinforced Poly (Lactic Acid) (Pla) As a Green Composites : Review, Int. J. Eng. Sci. Technol. 4 (2012) 4429–4439.
[119] M. Ejaz, M.M. Azad, A.U.R. Shah, S.K. Afaq, J.il Song, Mechanical and Biodegradable Properties of Jute/Flax Reinforced PLA Composites, Fibers Polym. 21 (2020) 2635–2641, https://doi.org/10.1007/s12221-020-1370-y.
[120] M.A. Sawpan, K.L. Pickering, A. Fernyhough, Improvement of mechanical performance of industrial hemp fibre reinforced polylactide biocomposites, Compos. Part A Appl. Sci. Manuf. 42 (2011) 310–319, https://doi.org/10.1016/j.compositesa.2010.12.004, https://doi.org/https://doi.org/.
[121] H. Anuar, A. Zuraida, J.G. Kovacs, T. Tabi, Improvement of mechanical properties of injection-molded polylactic acid-kenaf fiber biocomposite, J. Thermoplast. Compos. Mater. 25 (2012) 153–164, https://doi.org/10.1177/0892705711408984.
[122] H. Liu, H. He, X. Peng, B. Huang, J. Li, Three-dimensional printing of poly(lactic acid) bio-based composites with sugarcane bagasse fiber: Effect of printing orientation on tensile performance, Polym. Adv. Technol. (2019) 30, https://doi.org/10.1002/pat.4524.
[125] D.S K.L.P.M. Milosevic, Characterizing the Mechanical Properties of Fused Deposition Modelling Natural Fiber Recycled Polypropylene Composites, J. Compos. Sci. 1 (2017) 7, https://doi.org/10.3390/jcs1010007.
[126] Y. Yao, M. Li, M. Lackner, L. Herfried, A continuous fiber-reinforced additive manufacturing processing based on PET fiber and PLA, Materials (Basel). 13 (2020). https://doi.org/10.3390/ma13143044.
[127] H. Zhang, D. Liu, T. Huang, Q. Hu, H. Lammer, Three-dimensional printing of continuous flax fiber-reinforced thermoplastic composites by five-axis machine, Materials (Basel) 13 (2020), https://doi.org/10.3390/ma13071678.
[128] Q. Hu, Y. Duan, H. Zhang, D. Liu, B. Yan, F. Peng, Manufacturing and 3D printing of continuous carbon fiber prepreg filament, J. Mater. Sci. 53 (2018) 1887–1898, https://doi.org/10.1007/s10853-017-1624-2.
[129] H. Brooks, Title : 3D printing of continuous Kevlar fibre reinforced composites, 2019. https://www.researchgate.net/publication/336216483.
[130] C. Yang, X. Tian, T. Liu, Y. Cao, D. Li, 3D printing for continuous fiber reinforced thermoplastic composites: Mechanism and performance, Rapid Prototyp. J. 23 (2017) 209–215, https://doi.org/10.1108/RPJ-08-2015-0098.
[131] N. Li, Y. Li, S. Liu, Rapid prototyping of continuous carbon fiber reinforced polylactic acid composites by 3D printing, J. Mater. Process. Technol. 238 (2016) 218–225, https://doi.org/10.1016/j.jmatprotec.2016.07.025.
[132] H. Mei, Z. Ali, Y. Yan, I. Ali, L. Cheng, Influence of mixed isotropic fiber angles and hot press on the mechanical properties of 3D printed composites, Addit. Manuf. 27 (2019) 150–158, https://doi.org/10.1016/j.addma.2019.03.008.
[133] Mark Two The powerful professional Continuous Carbon Fiber 3D printer for aluminum-strength parts, (n.d.). https://markforged.com/3d-printers/mark-two (accessed October 15, 2020).
[134] R. Matsuzaki, M. Ueda, M. Namiki, T.K. Jeong, H. Asahara, K. Horiguchi, T. Nakamura, A. Todoroki, Y. Hirano, Three-dimensional printing of continuous-fiber composites by in-nozzle impregnation, Sci. Rep. 6 (2016) 1–7, https://doi.org/10.1038/srep23058.
[135] J. Suteja, H. Firmanto, A. Soesanti, C. Christian, Properties investigation of 3D printed continuous pineapple leaf fiber-reinforced PLA composite, J. Thermoplast. Compos. Mater. (2020), https://doi.org/10.1177/0892705720945371.
[136] A. Le Duigou, A. Barbé, E. Guillou, M. Castro, 3D printing of continuous flax fibre reinforced biocomposites for structural applications, Mater. Des. 180 (2019), 107884, https://doi.org/10.1016/j.matdes.2019.107884 https://doi.org/.
[137] J.I.N. Montalvo, M.A. Hidalgo, 3D printing with natural fiber reinforced filament, Proc. - 26th Annu. Int. Solid Free. Fabr. Symp. - An Addit. Manuf. Conf. SFF 2015. (2020) 922–934.
[138] A. Le Duigou, A. Barbé, E. Guillou, M. Castro, 3D printing of continuous flax fibre reinforced biocomposites for structural applications, Mater. Des. 180 (2019), 107884, https://doi.org/10.1016/j.matdes.2019.107884 https://doi.org/https://doi.org/.
[139] P. Cheng, K. Wang, X. Chen, J. Wang, Y. Peng, S. Ahzi, C. Chen, Interfacial and mechanical properties of continuous ramie fiber reinforced biocomposites

fabricated by in-situ impregnated 3D printing, Ind. Crops Prod. 170 (2021), 113760, https://doi.org/10.1016/j.indcrop.2021.113760.
[140] A.S. Jose, A. Athijayamani, S.P. Jani, A review on the mechanical properties of bio waste particulate reinforced polymer composites, Mater. Today Proc. 37 (2020) 1757–1760, https://doi.org/10.1016/j.matpr.2020.07.360.
[141] B.D.M. Matos, V. Rocha, E.J. da Silva, H.D.S. Barud, Evaluation of commercially available polylactic acid (PLA) filaments for 3D printing applications, Journal of Thermal Analysis and Calorimetry (2018) 137, https://doi.org/10.1007/s10973-018-7967-3.
[142] Senvol LLC, Senvol 3D Printing Materials Database, (n.d.). http://senvol.com/material-search/ (accessed July 15, 2020).
[143] M. Kariz, M. Sernek, M.K. Kuzman, Effect of humidity on 3D-printed specimens from wood-pla filaments, Wood Res 63 (2018) 917–922.
[144] Q. Wang, J. Sun, Q. Yao, C. Ji, J. Liu, Q. Zhu, 3D printing with cellulose materials, Cellulose 25 (2018) 4275–4301, https://doi.org/10.1007/s10570-018-1888-y.
[145] T.C. Yang, Effect of extrusion temperature on the physico-mechanical properties of unidirectional wood fiber-reinforced polylactic acid composite (WFRPC) components using fused depositionmodeling, Polymers (Basel) 10 (2018), https://doi.org/10.3390/polym10090976.
[146] M.K. Kuzman, N. Ayrilmis, M. Sernek, M. Kariz, Effect of selected printing settings on viscoelastic behaviour of 3D printed polymers with and without wood, Mater. Res. Express. 6 (2019), https://doi.org/10.1088/2053-1591/ab411c.
[147] N. Ayrilmis, Effect of layer thickness on surface properties of 3D printed materials produced from wood flour/PLA filament, Polym. Test. 71 (2018) 163–166, https://doi.org/10.1016/j.polymertesting.2018.09.009.
[148] J.V. Ecker, A. Haider, I. Burzic, A. Huber, G. Eder, S. Hild, Mechanical properties and water absorption behaviour of PLA and PLA/wood composites prepared by 3D printing and injection moulding, Rapid Prototyp. J. 25 (2019) 672–678, https://doi.org/10.1108/RPJ-06-2018-0149.
[149] N. Ayrilmis, M. Kariz, J.H. Kwon, M. Kitek Kuzman, Effect of printing layer thickness on water absorption and mechanical properties of 3D-printed wood/PLA composite materials, Int. J. Adv. Manuf. Technol. 102 (2019) 2195–2200, https://doi.org/10.1007/s00170-019-03299-9.
[150] S. Bhagia, R.R. Lowden, D. Erdman, M. Rodriguez, B.A. Haga, I.R.M. Solano, N. C. Gallego, Y. Pu, W. Muchero, V. Kunc, A.J. Ragauskas, Tensile properties of 3D-printed wood-filled PLA materials using poplar trees, Appl. Mater. Today. 21 (2020), 100832, https://doi.org/10.1016/j.apmt.2020.100832.
[151] S. Bhagia, K. Bornani, R. Agarwal, A. Satlewal, J. Ďurkovič, R. Lagaňa, M. Bhagia, C.G. Yoo, X. Zhao, V. Kunc, Y. Pu, S. Ozcan, A.J. Ragauskas, Critical review of FDM 3D printing of PLA biocomposites filled with biomass resources, characterization, biodegradability, upcycling and opportunities for biorefineries, Appl. Mater. Today. 24 (2021), 101078, https://doi.org/10.1016/j.apmt.2021.101078.
[152] S. Guessasma, S. Belhabib, H. Nouri, Microstructure and mechanical performance of 3D printed wood-PLA/PHA using fused deposition modelling: Effect of printing temperature, Polymers (Basel) 11 (2019), https://doi.org/10.3390/polym11111778.
[153] M. Kariz, M. Sernek, M. Obućina, M.K. Kuzman, Effect of wood content in FDM filament on properties of 3D printed parts, Mater. Today Commun. 14 (2018) 135–140, https://doi.org/10.1016/j.mtcomm.2017.12.016.
[154] K. Vigneshwaran, N. Venkateshwaran, Statistical analysis of mechanical properties of wood-PLA composites prepared via additive manufacturing, Int. J. Polym. Anal. Charact. 24 (2019) 584–596, https://doi.org/10.1080/1023666X.2019.1630940.
[155] J.M. Koo, J. Kang, S.H. Shin, J. Jegal, H.G. Cha, S. Choy, M. Hakkarainen, J. Park, D.X. Oh, S.Y. Hwang, Biobased thermoplastic elastomer with seamless 3D-Printability and superior mechanical properties empowered by in-situ polymerization in the presence of nanocellulose, Compos. Sci. Technol. 185 (2020), 107885, https://doi.org/10.1016/j.compscitech.2019.107885.
[156] P. Phanthong, P. Reubroycharoen, X. Hao, G. Xu, A. Abudula, G. Guan, Nanocellulose: Extraction and application, Carbon Resour. Convers. 1 (2018) 32–43, https://doi.org/10.1016/j.crcon.2018.05.004.
[157] R.J. Moon, A. Martini, J. Nairn, J. Simonsen, J. Youngblood, Cellulose nanomaterials review: structure{,} properties and nanocomposites, Chem. Soc. Rev. 40 (2011) 3941–3994, https://doi.org/10.1039/C0CS00108B.
[158] J. Dong, M. Li, L. Zhou, S. Lee, C. Mei, X. Xu, Q. Wu, The influence of grafted cellulose nanofibers and postextrusion annealing treatment on selected properties of poly(lactic acid) filaments for 3D printing, J. Polym. Sci. Part B Polym. Phys. 55 (2017) 847–855, https://doi.org/10.1002/polb.24333.
[159] D. Rigotti, A. Dorigato, A. Cataldi, L. Fambri, A. Pegoretti, Nanocellulose as reinforcing agent for biodegradable polymers in 3D printing fused deposition modeling, ECCM 2018 - 18th Eur, Conf. Compos. Mater. (2020) 24–28.
[160] A.N. Frone, D. Batalu, I. Chiulan, M. Oprea, A.R. Gabor, C.A. Nicolae, V. Raditoiu, R. Trusca, D.M. Panaitescu, Morpho-structural, thermal and mechanical properties of PLA/PHB/Cellulose biodegradable nanocomposites obtained by compression molding, extrusion, and 3d printing, Nanomaterials (2020) 10, https://doi.org/10.3390/nano10010051.
[161] L. Li, Y. Chen, T. Yu, N. Wang, C. Wang, H. Wang, Preparation of polylactic acid/TEMPO-oxidized bacterial cellulose nanocomposites for 3D printing via Pickering emulsion approach, Compos. Commun. 16 (2019) 162–167, https://doi.org/10.1016/j.coco.2019.10.004.
[162] H.L. Tekinalp, X. Meng, Y. Lu, V. Kunc, L.J. Love, W.H. Peter, S. Ozcan, High modulus biocomposites via additive manufacturing: Cellulose nanofibril networks as “microsponges, Compos. Part B Eng. 173 (2019), 106817, https://doi.org/10.1016/j.compositesb.2019.05.028.
[163] T. Ambone, A. Torris, K. Shanmuganathan, Enhancing the mechanical properties of 3D printed polylactic acid using nanocellulose, Polym. Eng. Sci. (2020) 1842–1855, https://doi.org/10.1002/pen.25421.
[164] D. Mohan, Z.K. Teong, A.N. Bakir, M.S. Sajab, H. Kaco, Extending cellulose-based polymers application in additive manufacturing technology: A review of recent approaches, Polymers (Basel) 12 (2020), https://doi.org/10.3390/POLYM12091876.
[165] M. Ghasemlou, F. Daver, E.P. Ivanova, Y. Habibi, B. Adhikari, Surface modifications of nanocellulose: From synthesis to high-performance nanocomposites, Prog. Polym. Sci. 119 (2021), 101418, https://doi.org/10.1016/j.progpolymsci.2021.101418.
[166] M.E. Lamm, L. Wang, V. Kishore, H. Tekinalp, V. Kunc, J. Wang, D.J. Gardner, S. Ozcan, Material Extrusion Additive Manufacturing of Wood and Lignocellulosic Filled Composites, (n.d.). 2022.
[167] H. Talebi, F.A. Ghasemi, A. Ashori, The effect of nanocellulose on mechanical and physical properties of chitosan-based biocomposites, J. Elastomers Plast. 54 (2022) 22–41, https://doi.org/10.1177/00952443211017169.
[168] Z. Tang, C. Zhang, X. Liu, The crystallization behavior and mechanical properties of polylactic acid in the presence of a crystal nucleating agent, J. Appl. Polym. Sci. (2012) 125, https://doi.org/10.1002/app.34799.
[169] J. Dai, Q. Yang, B. Liu, Crystallization Behavior of PLA/PEG/Nucleating Agent Blends, Adv. Mater. Res. 807–809 (2013) 578–581, https://doi.org/10.4028/www.scientific.net/AMR.807-809.578.
[170] L. Aliotta, P. Cinelli, M. Coltelli, M.C. Righetti, M. Gazzano, A. Lazzeri, Effect of nucleating agents on crystallinity and properties of Poly (lactic acid) (PLA), Eur. Polym. J. (2017), https://doi.org/10.1016/j.eurpolymj.2017.04.041.
[171] N.P. Levenhagen, M.D. Dadmun, Bimodal molecular weight samples improve the isotropy of 3D printed polymeric samples, Polymer (Guildf) 122 (2017) 232–241, https://doi.org/10.1016/j.polymer.2017.06.057.
[172] S. Shaffer, K. Yang, J. Vargas, M.A. Di Prima, W. Voit, On reducing anisotropy in 3D printed polymers via ionizing radiation, Polymer (Guildf) 55 (2014) 5969–5979, https://doi.org/10.1016/j.polymer.2014.07.054.
[173] C.H. Lee, A. Khalina, S.H. Lee, Importance of interfacial adhesion condition on characterization of plant-fiber-reinforced polymer composites: A review, Polymers (Basel) 13 (2021) 1–22, https://doi.org/10.3390/polym13030438.
[174] E. Petinakis, L. Yu, G. Edward, K. Dean, H. Liu, A.D. Scully, Effect of matrix-particle interfacial adhesion on the mechanical properties of poly(lactic acid)/wood-flour micro-composites, J. Polym. Environ. 17 (2009) 83–94, https://doi.org/10.1007/s10924-009-0124-0.
[175] M. Hao, H. Wu, F. Qiu, X. Wang, Interface bond improvement of sisal fibre reinforced polylactide composites with added epoxy oligomer, Materials (Basel) 11 (2018), https://doi.org/10.3390/ma11030398.
[176] C.A. Fuentes Rojas, Interfacial Adhesion in Natural and Synthetic Fibre Composites: a Physical-Chemical-Mechanical Approach, 2014. https://doi.org/10.13140/RG.2.2.36823.52647.
[177] E. LARA-CURZIO, 4.18 - Properties of CVI–SiC Matrix Composites, in: A. Kelly, C. Zweben (Eds.), Compr. Compos. Mater, Pergamon, Oxford, 2000, pp. 533–577, https://doi.org/https://doi.org/10.1016/B0-08-042993-9/00112-1.
[178] K. Olonisakin, M. fan, Z. Xin-Xiang, L. Ran, W.S. Lin, W. Zhang, Y. Wenbin, Key Improvements in Interfacial Adhesion and Dispersion of Fibers/Fillers in Polymer Matrix Composites; Focus on PLA Matrix Composites, Compos. Interfaces. 00 (2021) 1–50, https://doi.org/10.1080/09276440.2021.1878441.
[179] M.S. Singhvi, S.S. Zinjarde, D.V. Gokhale, Polylactic acid: synthesis and biomedical applications, J. Appl. Microbiol. 127 (2019) 1612–1626, https://doi.org/10.1111/jam.14290.
[180] M. Bayart, K. Adjallé, A. Diop, P. Ovlaque, S. Barnabé, M. Robert, S. Elkoun, PLA/flax fiber bio-composites: effect of polyphenol-based surface treatment on interfacial adhesion and durability, Compos. Interfaces. 28 (2020) 1–22, https://doi.org/10.1080/09276440.2020.1773179.
[181] R. Siakeng, M. Jawaid, M. Asim, N. Saba, M.R. Sanjay, S. Siengchin, H. Fouad, Alkali treated coir/pineapple leaf fibres reinforced pla hybrid composites: Evaluation of mechanical, morphological, thermal and physical properties, Express Polym. Lett. 14 (2020) 717–730, https://doi.org/10.3144/expresspolymlett.2020.59.
[182] Z. Yang, X. Feng, M. Xu, D. Rodrigue, Properties of poplar fiber/PLA composites: Comparison on the effect of maleic anhydride and KH550 modification of poplar fiber, Polymers (Basel) 12 (2020) 1–13, https://doi.org/10.3390/polym12030729.
[183] P. Ramesh, B.D. Prasad, K.L. Narayana, Influence of Montmorillonite Clay Content on Thermal, Mechanical, Water Absorption and Biodegradability Properties of Treated Kenaf Fiber/PLA-Hybrid Biocomposites, Silicon 13 (2021) 109–118, https://doi.org/10.1007/s12633-020-00401-9.
[184] J. Khieomuang, C. Thongpin, Fabrication of non-woven hybrid natural fiber/poly (lactic acid) composite via prepreg lamination, IOP Conf. Ser. Mater. Sci. Eng. (2020) 965, https://doi.org/10.1088/1757-899X/965/1/012017.
[185] F.J. Li, X.T. Yu, Z. Huang, D.F. Liu, Interfacial improvements in cellulose nanofibers reinforced polylactide bionanocomposites prepared by in situ reactive extrusion, Polym. Adv. Technol. 32 (2021) 2352–2366, https://doi.org/10.1002/pat.5264.
[186] Y. Yin, L.A. Lucia, L. Pal, X. Jiang, M.A. Hubbe, Lipase-catalyzed laurate esterification of cellulose nanocrystals and their use as reinforcement in PLA composites, Cellulose 27 (2020) 6263–6273, https://doi.org/10.1007/s10570-020-03225-3.
[187] J.H. Lee, S.H. Park, S.H. Kim, Surface alkylation of cellulose nanocrystals to enhance their compatibility with polylactide, Polymers (Basel) 12 (2020) 1–16, https://doi.org/10.3390/polym12010178.

[188] H. Jing, H. He, H. Liu, B. Huang, C. Zhang, Study on properties of polylactic acid/lemongrass fiber biocomposites prepared by fused deposition modeling, Polym. Compos. 42 (2021) 973–986, https://doi.org/10.1002/pc.25879.
[189] F.Y. Wang, L. Dai, T.T. Ge, C.B. Yue, Y.M. Song, A-Methylstyrene-Assisted Maleic Anhydride Grafted Poly(Lactic Acid) As an Effective Compatibilizer Affecting Properties of Microcrystalline Cellulose/Poly(Lactic Acid) Composites, Express Polym. Lett. 14 (2020) 530–541, https://doi.org/10.3144/expresspolymlett.2020.43.
[190] J. Liao, N. Brosse, S. Hoppe, G. Du, X. Zhou, A. Pizzi, One-step compatibilization of poly(lactic acid) and tannin via reactive extrusion, Mater. Des. 191 (2020), 108603, https://doi.org/10.1016/j.matdes.2020.108603.
[191] A. Arbelaiz, U. Txueka, I. Mezo, A. Orue, Biocomposites Based on Poly(Lactic Acid) Matrix and Reinforced with Lignocellulosic Fibers: The Effect of Fiber Type and Matrix Modification, J. Nat. Fibers. (2020) 1–14, https://doi.org/10.1080/15440478.2020.1726247, 00.
[192] B.M. Trinh, E.O. Ogunsona, T.H. Mekonnen, Thin-structured and compostable wood fiber-polymer biocomposites: Fabrication and performance evaluation, Compos. Part A Appl. Sci. Manuf. 140 (2021), 106150, https://doi.org/10.1016/j.compositesa.2020.106150.
[193] N.R. Rajendran Royan, J.S. Leong, W.N. Chan, J.R. Tan, Z.S.B. Shamsuddin, Current state and challenges of natural fibre-reinforced polymer composites as feeder in fdm-based 3d printing, Polymers (Basel) 13 (2021), https://doi.org/10.3390/polym13142289.
[194] S. Guessasma, S. Belhabib, H. Nouri, Understanding the microstructural role of bio-sourced 3D printed structures on the tensile performance, Polym. Test. (2019) 77, https://doi.org/10.1016/j.polymertesting.2019.105924.
[195] J. George, E.T.J. Klompen, T. Peijs, Thermal degradation of green and upgraded flax fibres, Adv. Compos. Lett. 10 (2001) 81–88, https://doi.org/10.1177/096369350101000205.
[196] V. Figueroa-Velarde, T. Diaz-Vidal, E.O. Cisneros-López, J.R. Robledo-Ortiz, E. J. López-Naranjo, P. Ortega-Gudiño, L.C. Rosales-Rivera, Mechanical and Physicochemical Properties of 3D-Printed Agave Fibers/Poly(lactic) Acid Biocomposites, Materials (Basel). 14 (2021) 3111, https://doi.org/10.3390/ma14113111.
[197] Q. Sun, G. Rizvi, C. Bellehumeur, P. Gu, Effect of processing conditions on the bonding quality of FDM polymer filaments, Rapid Prototyp. J. 14 (2008) 72–80, https://doi.org/10.1108/13552540810862028.
[198] C. Bellehumeur, L. Li, Q. Sun, P. Gu, Modeling of Bond Formation Between Polymer Filaments in the Fused Deposition Modeling Process, J. Manuf. Process. 6 (2004) 170–178, https://doi.org/10.1016/S1526-6125(04)70071-7, https://doi.org/https://doi.org/.
[199] N. Sabyrov, A. Abilgaziyev, M.H. Ali, Enhancing interlayer bonding strength of FDM 3D printing technology by diode laser-assisted system, Int. J. Adv. Manuf. Technol. 108 (2020) 603–611, https://doi.org/10.1007/s00170-020-05455-y.
[200] A.K. Ravi, A. Deshpande, K.H. Hsu, An in-process laser localized pre-deposition heating approach to inter-layer bond strengthening in extrusion based polymer additive manufacturing An in-process laser localized pre-deposition heating approach to inter-layer bond strengthening in extrusion, J. Manuf. Process. 24 (2016) 179–185, https://doi.org/10.1016/j.jmapro.2016.08.007.
[201] V. Kishore, C. Ajinjeru, A. Nycz, B. Post, J. Lindahl, V. Kunc, C. Duty, Infrared preheating to improve interlayer strength of big area additive manufacturing (BAAM) components, Addit. Manuf. 14 (2017) 7–12, https://doi.org/10.1016/j.addma.2016.11.008.
[202] Y. Liao, C. Liu, B. Coppola, G. Barra, L. Di Maio, L. Incarnato, K. Lafdi, Effect of Porosity and Crystallinity on 3D Printed PLA Properties, Polymers (Basel) 11 (2019), https://doi.org/10.3390/polym11091487.
[203] L. Jiang, T. Shen, P. Xu, X. Zhao, X. Li, W. Dong, P. Ma, M. Chen, Crystallization modification of poly(lactide) by using nucleating agents and stereocomplexation, E-Polymers. 16 (2016) 1–13. https://doi.org/doi:10.1515/epoly-2015-0179.
[204] S. Farah, D.G. Anderson, R. Langer, Physical and mechanical properties of PLA, and their functions in widespread applications — A comprehensive review, Adv. Drug Deliv. Rev. 107 (2016) 367–392, https://doi.org/10.1016/j.addr.2016.06.012.
[205] A. Nassar, M. Younis, M. Elzareef, E. Nassar, Effects of heat-treatment on tensile behavior and dimension stability of 3d printed carbon fiber reinforced composites, Polymers (Basel) 13 (2021) 1–21, https://doi.org/10.3390/polym13244305.
[206] J. Butt, R. Bhaskar, Investigating the effects of annealing on the mechanical properties of FFF-printed thermoplastics, J. Manuf. Mater. Process. 4 (2020) 1–20, https://doi.org/10.3390/jmmp4020038.
[207] R. Wach, P. Wolszczak, A. Adamus-Włodarczyk, Enhancement of Mechanical Properties of FDM-PLA Parts via Thermal Annealing, Macromol. Mater. Eng. (2018) 303, https://doi.org/10.1002/mame.201800169.
[208] J. Suder, Z. Bobovsky, Z. Zeman, J. Mlotek, M. Vocetka, The influence of annealing temperature on tensile strength of polylactic acid, MM Sci. J. 2020 (2020) 4132–4137, https://doi.org/10.17973/MMSJ.2020_11_2020048.
[209] J. Hu, Y. Zhu, H. Huang, J. Lu, Recent advances in shape-memory polymers: Structure, mechanism, functionality, modeling and applications, Prog. Polym. Sci. 37 (2012) 1720–1763, https://doi.org/10.1016/j.progpolymsci.2012.06.001.
[210] S. Valvez, P.N.B. Reis, L. Susmel, F. Berto, Fused filament fabrication-4d-printed shape memory polymers: A review, Polymers (Basel) 13 (2021) 1–25, https://doi.org/10.3390/polym13050701.
[211] M. Barletta, A. Gisario, M. Mehrpouya, 4D printing of shape memory polylactic acid (PLA) components: Investigating the role of the operational parameters in fused deposition modelling (FDM), J. Manuf. Process. 61 (2021) 473–480, https://doi.org/10.1016/j.jmapro.2020.11.036.
[212] M. Mehrpouya, A. Azizi, S. Janbaz, A. Gisario, Investigation on the Functionality of Thermoresponsive Origami Structures, Adv. Eng. Mater. 22 (2020) 1–6, https://doi.org/10.1002/adem.202000296.
[213] M. Mehrpouya, A. Gisario, A. Azizi, M. Barletta, Investigation on shape recovery of 3D printed honeycomb sandwich structure, Polym. Adv. Technol. (2020) 1–5, https://doi.org/10.1002/pat.5020.
[214] T. van Manen, S. Janbaz, K.M.B. Jansen, A.A. Zadpoor, 4D printing of reconfigurable metamaterials and devices, Commun. Mater. 2 (2021), https://doi.org/10.1038/s43246-021-00165-8.
[215] T. Langford, A. Mohammed, K. Essa, A. Elshaer, H. Hassanin, 4D Printing of Origami Structures for Minimally Invasive Surgeries Using Functional Scaffold, Appl. Sci. 11 (2021) 1–13, https://doi.org/10.3390/app11010332.
[216] G. Singh, S. Singh, C. Prakash, R. Kumar, R. Kumar, S. Ramakrishna, Characterization of three-dimensional printed thermal-stimulus polylactic acid-hydroxyapatite-based shape memory scaffolds, Polym. Compos. 41 (2020) 3871–3891, https://doi.org/10.1002/pc.25683.
[217] A. Le Duigou, M. Castro, R. Bevan, N. Martin, 3D printing of wood fibre biocomposites: From mechanical to actuation functionality, Mater. Des. 96 (2016) 106–114, https://doi.org/10.1016/j.matdes.2016.02.018.
[218] D. Correa, A. Papadopoulou, C. Guberan, N. Jhaveri, S. Reichert, A. Menges, S. Tibbits, 3D-Printed Wood: Programming Hygroscopic Material Transformations, 3D Print, Addit. Manuf. 2 (2015) 106–116, https://doi.org/10.1089/3dp.2015.0022.
[219] A.Le Duigou, M. Castro, Hygromorph BioComposites, Effect of fibre content and interfacial strength on the actuation performances, Ind. Crops Prod. 99 (2017) 142–149, https://doi.org/10.1016/j.indcrop.2017.02.004.
[220] B.G. J.D.E. Vazquez, Designing for Shape Change: A Case Study on 3D Printing Composite Materials for Responsive Architectures, in: Conference, 2019 http://papers.cumincad.org/data/works/att/caadria2019_379.pdf.
[221] T. Cheng, M. Thielen, S. Poppinga, Y. Tahouni, D. Wood, T. Steinberg, A. Menges, T. Speck, Bio-Inspired Motion Mechanisms: Computational Design and Material Programming of Self-Adjusting 4D-Printed Wearable Systems, Adv. Sci. 8 (2021) 1–12, https://doi.org/10.1002/advs.202100411.
[222] A. Papadopoulou, C. Guberan, N. Jhaveri, D. Correa, 3D-Printed Wood : Programming Hygroscopic Material Transformations 2 (2015) 106–116, https://doi.org/10.1089/3dp.2015.0022.
[223] A.Le Duigou, M. Castro, Evaluation of force generation mechanisms in natural, passive hydraulic actuators, Sci. Rep. 6 (2016) 1–9, https://doi.org/10.1038/srep18105.
[224] R.L. Lincoln, F. Scarpa, V.P. Ting, R.S. Trask, Multifunctional composites: A metamaterial perspective, Multifunct. Mater. 2 (2019), https://doi.org/10.1088/2399-7532/ab5242.
[225] S. Poppinga, D. Correa, B. Bruchmann, A. Menges, T. Speck, Plant movements as concept generators for the development of biomimetic compliant mechanisms, Integr. Comp. Biol. 60 (2020) 886–895, https://doi.org/10.1093/icb/icaa028.